

Oryza CLIMtools: A genome–environment association resource reveals adaptive roles for heterotrimeric G proteins in the regulation of rice agronomic traits

Ángel Ferrero-Serrano^{1,*}, David Chakravorty¹, Kobi J. Kirven² and Sarah M. Assmann^{1,*}

¹Biology Department, Pennsylvania State University, 208 Mueller Laboratory, University Park, PA 16802, USA

²Intercollege Graduate Degree Program in Bioinformatics and Genomics, Pennsylvania State University, 208 Mueller Laboratory, University Park, PA 16802, USA

*Correspondence: Ángel Ferrero-Serrano (aaf11@psu.edu), Sarah M. Assmann (sma3@psu.edu)

<https://doi.org/10.1016/j.xplc.2024.100813>

ABSTRACT

Modern crop varieties display a degree of mismatch between their current distributions and the suitability of the local climate for their productivity. To address this issue, we present Oryza CLIMtools (https://gramene.org/CLIMtools/orzaya_v1.0/), the first resource for pan-genome prediction of climate-associated genetic variants in a crop species. Oryza CLIMtools consists of interactive web-based databases that enable the user to (1) explore the local environments of traditional rice varieties (landraces) in South-East Asia and (2) investigate the environment by genome associations for 658 Indica and 283 Japonica rice landrace accessions collected from georeferenced local environments and included in the 3K Rice Genomes Project. We demonstrate the value of these resources by identifying an interplay between flowering time and temperature in the local environment that is facilitated by adaptive natural variation in *OsHD2* and disrupted by a natural variant in *OsSOC1*. Prior quantitative trait locus analysis has suggested the importance of heterotrimeric G proteins in the control of agronomic traits. Accordingly, we analyzed the climate associations of natural variants in the different heterotrimeric G protein subunits. We identified a coordinated role of G proteins in adaptation to the prevailing potential evapotranspiration gradient and revealed their regulation of key agronomic traits, including plant height and seed and panicle length. We conclude by highlighting the prospect of targeting heterotrimeric G proteins to produce climate-resilient crops.

Key words: *Oryza sativa*, rice, G by E, adaptation, flowering time, GWAS, *OsHD2*, *OsSOC1*, heterotrimeric G protein, *OsRGA1*, *d1*, *OsGS3*, *OsDEP1*, *OsGGC2*

Ferrero-Serrano Á., Chakravorty D., Kirven K.J., and Assmann S.M. (2024). Oryza CLIMtools: A genome–environment association resource reveals adaptive roles for heterotrimeric G proteins in the regulation of rice agronomic traits. *Plant Comm.* **5**, 100813.

INTRODUCTION

As the dietary staple of over half of the world's population, rice is arguably the most critical food source on the planet (Bin Rahman and Zhang, 2023). The Green Revolution was crucial to promoting food security worldwide in the late 20th century, despite the concurrent increase in demand for food as a result of exponential growth of the world's population (Dalrymple, 1986). As farmers began to prioritize high-yielding crops, they often abandoned local crop varieties (Frankel, 1974), resulting in the loss of genetic diversity over time that characterizes modern rice varieties (Khoury et al., 2022). Selective breeding practices in crops have primarily prioritized high-yielding but genetically uniform varieties, which can reduce adaptive potential

(Østerberg et al., 2017). Therefore, as crop diversity decreases, so does resilience to extreme weather events such as heatwaves, droughts, and floods, which are becoming more frequent owing to the already noticeable effects of climate change and are predicted to reduce crop yields globally (Food and Agriculture Organization of the United Nations et al., 2018). To promote global food security, crop production can be stabilized by increasing genetic diversity (Renard and Tilman, 2019). A promising approach is to restore to modern elite

Published by the Plant Communications Shanghai Editorial Office in association with Cell Press, an imprint of Elsevier Inc., on behalf of CSPB and CEMPS, CAS.

varieties the lost genetic diversity present in local varieties (landraces) that are adapted to the local climate, thereby fostering improved yield stability under diverse conditions (McNally et al., 2009; Lasky et al., 2015; Faye et al., 2019).

The 3000 (3K) Rice Genome Project has provided high-quality sequencing data for 3010 rice genomes obtained using Illumina-based next-generation sequencing (3000 Rice Genomes Project, 2014; Wang et al., 2018). Indica and Japonica are the two main subspecies of Asian cultivated rice and are the products of two separate domestication events from the ancestral species *Oryza rufipogon* (Kato, 1930; Sweeney and McCouch, 2007). The 3K dataset provides information on the genetic diversity of 658 Indica and 283 Japonica landraces grown in South-East Asia (Figure 1), whose collection sites are known and whose population structure and history have been described (Gutaker et al., 2020). By studying local landraces, researchers can explore the factors that have shaped rice diversity and identify genetic variants and traits associated with the local environment that are suggestive of local adaptation. This information can aid the development of new high-yielding rice varieties better adapted to anthropogenically altered climates to improve food security and sustainability.

Our recent work on locally adapted accessions of *Arabidopsis thaliana*, collected from their local habitats, identified genome-wide associations between their natural genetic variation and a myriad of geoenvironmental variables that define each local habitat. *Arabidopsis* CLIMtools provides a resource with which the community can explore these associations (Ferrero-Serrano and Assmann, 2019; Ferrero-Serrano et al., 2022). However, similar resources have not previously been available for any crop species. Here, we present the first resource to provide gene-by-phenotype-by-environment associations to assist with rice research and breeding programs. We integrate datasets comprising 413 geoenvironmental variables that define local environmental conditions at the collection sites of 941 landraces and make this information available in OryzaCLIM (https://gramene.org/CLIMtools/oryza_v1.0/OryzaCLIM/). Using this environmental dataset, we establish an adaptive relationship between flowering time and the minimum temperature of the coldest month for Indica and Japonica landraces. In addition, we present an interactive dataset of genotype–environment associations for 658 Indica and 283 Japonica rice landraces, with detailed information on the genes and variants statistically associated with the 413 environmental variables. These results are publicly available in a database platform, Oryza CLIMtools, available at the Gramene portal (Gramene.org; Tello-Ruiz et al., 2021). Oryza CLIMtools enables users to identify candidate adaptive genetic variants related to a given environmental variable of interest as codified in Oryza CLIMGeno and, conversely, to identify in Oryza GenoCLIM environmental variables associated with variation at any genetic locus of interest. We demonstrate the use of these tools, revealing an interplay among plant height, panicle length, and seed length that is associated with potential evapotranspiration (PET) in the local environment and depends on both natural variation in the heterotrimeric G protein $G\alpha$ subunit gene, *OsRGA1*, and a single nucleotide polymorphism (SNP) that introduces a premature stop codon in the $G\gamma$ gene *OsGS3*.

RESULTS

Oryza CLIMtools

We created a comprehensive database of environmental data on rice landraces to serve as a valuable resource for researchers aiming to enhance rice research by integrating environmental parameters. This suite of online resources facilitates the process of incorporating environmental data into studies and provides a user-friendly interface through which researchers can access and utilize this information. Oryza CLIMtools (Figure 1) comprises three interactive web-based databases, OryzaCLIM, Oryza GenoCLIM, and Oryza CLIMGeno, that enable users to explore associations of promoter and transcript natural variants in 941 rice landraces collected from their native range with 413 geoenvironmental variables that define the environmental conditions in their collection areas (Figure 1). These environmental variables are collated in our OryzaCLIM tool and characterize the local environments of 658 Indica and 283 Japonica georeferenced and fully sequenced landrace varieties included in the 3K Rice Genome Project (Gutaker et al., 2020; Figure 1; Supplemental Tables 1 and 2).

With Oryza CLIMtools (Figure 1), users can search for significant associations (false discovery rate [FDR] < 0.01) based on any climate parameter of interest using Oryza CLIMGeno. Alternatively, users can easily search for gene–climate associations (FDR < 0.01) based on any specific rice gene of interest using Oryza GenoCLIM. We also provide riboSNitch predictions, which indicate the likelihood that a variant alters RNA structure, as this is a mechanism for differential post-transcriptional regulation (Halvorsen et al., 2010). As shown by our analyses in *Arabidopsis* (Ferrero-Serrano et al., 2022), riboSNitches are a fruitful topic for investigation.

We encourage users of Oryza CLIMtools to read the “considerations and limitations” document that we make available in Oryza GenoCLIM and CLIMGeno to familiarize themselves with the particularities of this approach and the effects that aspects such as population structure or geographic distribution of the sampled population have on the interpretation of our results.

Oryza CLIMtools has the potential to assist the scientific community in ways that include:

- (1) Informing the choice of cultivars for experimental genome-wide association (GWA) analysis to facilitate inclusion of varieties from contrasting environments
- (2) Assigning relationships between phenotypic variability and environmental variation in this set of sequenced landraces, which can inform future studies of the functional interplay between genes and environments
- (3) Identifying the association of a particular environmental variable with variation in particular genes which, among other uses, may expedite forward genetics research
- (4) Identifying the association of genetic variation in specific genes of interest with environmental gradients which, among other uses, may expedite reverse genetics research

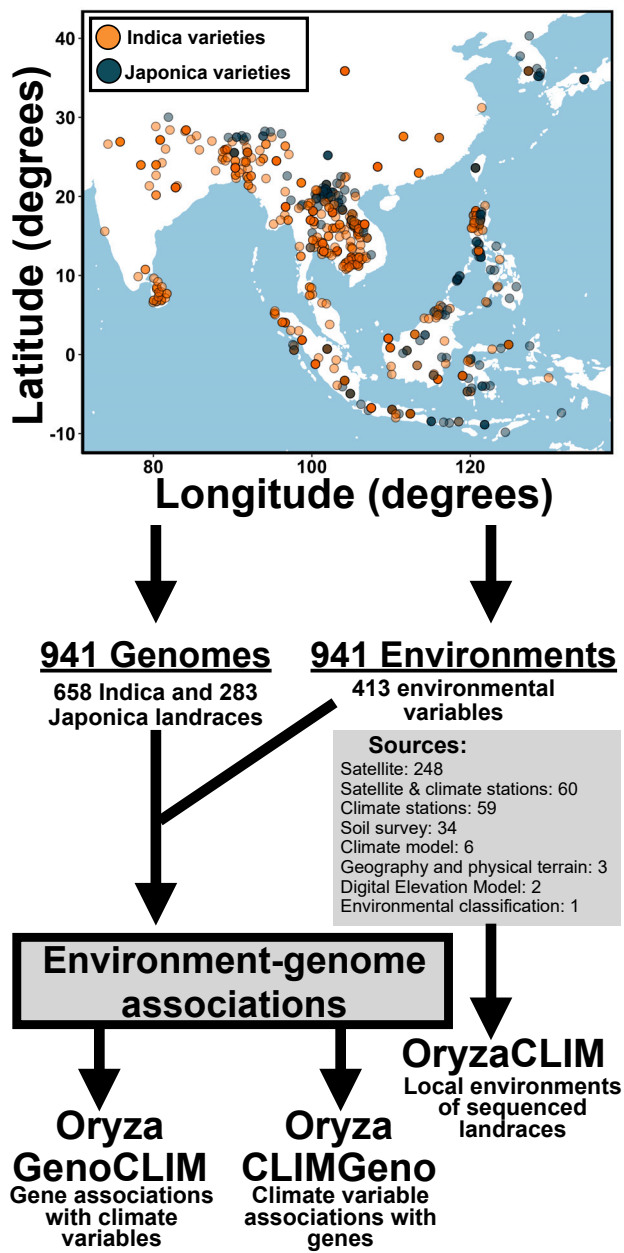


Figure 1. Global landrace distribution and environmental variables defining the local environments of the 941 fully sequenced Indica and Japonica varieties used in this study to create the three components of Oryza CLIMtools.

Geographic distribution of 658 Indica (orange data points) and 283 Japonica (blue data points) landrace varieties with known collection sites sequenced as part of the 3K Rice Genome Project (Wang et al., 2018; Gutaker et al., 2020). We curated 413 geoenvironmental variables that describe the local environments of these landraces. Oryza CLIMtools comprises a suite of online resources that provides gene-by-phenotype-by-environment associations to assist rice research and breeding programs.

We next illustrate the utility of these tools by (1) exploring the genetic basis of the interplay between flowering time and temperature in the local environment and (2) identifying a coordinated role of G proteins in adaptation to the local climate through regulation of key agronomic traits.

Natural variation in *OsHD2* and *OsSOC1* influences the flowering-time–temperature relationship

To support the use of landraces to uncover the genetic basis of local adaptation, we asked whether there was an association between the phenotypic characteristics of these varieties and the environmental characteristics of the areas where they are grown. Using the environmental dataset provided in OryzaCLIM, we revealed a positive relationship in Indica and Japonica landrace varieties between flowering time as documented in publicly available data (Mansueto et al., 2017) and the minimum temperature of the coldest month (Karger et al., 2017) typical of their local environment (Figure 2). This relationship between flowering time and temperature was particularly strong in Japonica landraces (Figure 2). To uncover the genetic basis of this adaptive trait, we used Oryza CLIMGeno and identified in these Japonica landraces a haplotype consisting of a set of one missense and six intronic covarying SNPs (Figure 2A) in *HEADING DATE 2* (*OsHD2/OsPRR37/Ghd7.1/DTH7*; *Os07g0695100*), which was associated with the minimum temperature of the coldest month (Figure 2B). Landraces with the haplotype version that is less frequent in the Japonica population (minor allele) are typically grown in colder locations and display early flowering. By contrast, late-flowering landraces with the haplotype version that is more frequent in the Japonica population (major allele) are typically from warmer areas (Wilcoxon test, $p < 0.0001$; Figure 2B).

To uncover the genetic basis of flowering-time adaptation to local temperature in Indica varieties, we used Oryza CLIMGeno and identified an association of an intronic variant in the floral pathway integrator and MADS-domain transcription factor *SUPPRESSOR OF OVEREXPRESSION OF CONSTANS1* (*OsSOC1/AGL20/OsMAD50*; *Os03g0122600*; Figure 2C) with the minimum temperature of the coldest month in Indica landraces (Figure 2D). The minor allele of *OsSOC1* is found in landraces that are typically grown in warmer areas and exhibit early flowering (Wilcoxon test, $p < 0.0001$; Figure 2D). This relationship disrupts the overall strength of the association between flowering time and temperature in the local environment ($R^2 = 0.22$, Figure 2B), which is stronger in the absence of the minor allele of *OsSOC1* ($R^2 = 0.26$). From these findings, we hypothesize that the early-flowering phenotype associated with the minor allele of *OsSOC1* may have been selected to favor flowering-time stability and thus sustained yields across multiple locations. To test this hypothesis, we calculated the difference in flowering time for 576 Indica landraces with publicly available records from two planting locations (Figure 2E), one in Hainan (China) and the other in Los Baños (Philippines) (Mansueto et al., 2017; Wang et al., 2020). The difference in flowering time between locations was calculated by subtracting the days to flowering in Hainan from the days to flowering in Los Baños. In support of the conclusion that later flowering is typical of landraces collected from warmer climates (Figure 2B and 2D), most landraces flowered later in the warmer location of Los Baños than in Hainan (Figure 2F). In addition, the flowering times of landrace varieties harboring the minor *OsSOC1* variant remained remarkably stable when planted in these two locations (Wilcoxon test, $p < 0.0001$; Figure 2F; note the reduced spread of data points

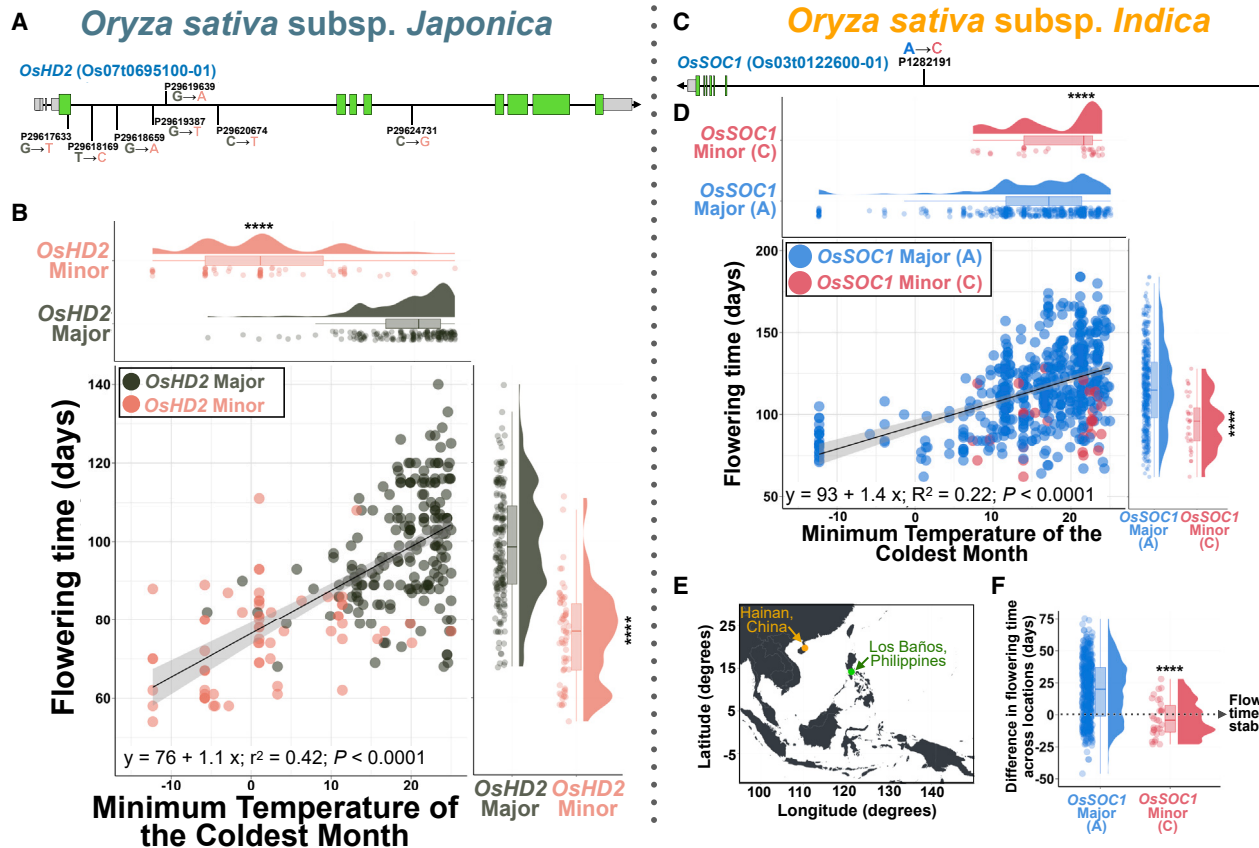


Figure 2. Natural variation in *OsHD2* tunes the relationship between heading date and temperature to the local environment; a minor variant of *SOC1* disrupts it.

(A) We identified in Japonica landraces an allele consisting of a set of one missense and six intronic covarying SNPs in *HEADING DATE 2* (*OsHD2*/Os_{PRR37}/Ghd7.1/DTH7; Os07g0695100). Gray indicates UTRs, green indicates exons, and black indicates introns.

(B) Flowering time in Japonica landraces is significantly associated with the minimum temperature of the coldest month for their local environment ($R^2 = 0.42$). Raincloud plots illustrate significantly different probability densities of the association of the local environment with flowering time for the major and minor alleles of *OsHD2* depicted in **(A)**. Coral data points and distributions represent landraces with the minor allele of *OsHD2*. Dark-gray data points and distributions represent landraces with the major allele of *OsHD2*.

(C) We identified in Indica landraces an intronic variant in the floral pathway integrator and MADS-domain transcription factor *SUPPRESSOR OF OVEREXPRESSION OF CONSTANS1* (*OsSOC1*/AGL20/OsMAD50; Os03g0122600). **(D)** Flowering time in Indica landraces, like that of Japonica landraces, is significantly associated with the minimum temperature of the coldest month for their local environment ($R^2 = 0.22$). Raincloud plots illustrate significantly different probability densities of the association of the local environment with flowering time for the major and minor alleles of the intronic SNP in *OsSOC1* depicted in **(A)**. Red data points and distributions represent landraces with the minor allele of *OsSOC1*. Blue data points and distributions represent landraces with the major allele of *OsSOC1*.

(E) Planting sites in Hainan (China) and Los Baños (Philippines) of 576 Indica landraces with flowering-time records at both of these locations in publicly available datasets retrieved from the Functional and Genomic Breeding (RFGB 2.0; Wang et al., 2020) and SNPseek (Mansueto et al., 2017) resource sites.

(F) Raincloud plot illustrating the significant flowering-time stability of Indica landraces harboring the minor allele of *OsSOC1* when planted at different locations. The difference in flowering time was calculated by subtracting the number of days to flowering for landraces in Hainan (China) from the days to flowering in Los Baños (Philippines). The positive values for most landraces indicate that they flowered later at lower latitudes in Los Baños relative to those in Hainan. In the boxplots, the lower and upper boundaries indicate the 25th and 75th percentile, respectively. The whisker below the box indicates the smallest value within 1.5 \times the interquartile range (IQR) below the 25th percentile. The whisker above the box indicates the largest value within 1.5 \times the IQR above the 75th percentile. The black line inside the box indicates the median. Pairwise non-parametric Wilcoxon tests were performed to assess differences between alleles. **** $p < 0.0001$; *** $0.0001 < p < 0.001$; ** $0.001 < p < 0.01$; * $0.01 < p < 0.05$; non-significant comparisons (ns) ($p > 0.05$). The associations between temperature and flowering time were fitted to a linear model. Regression lines are shown in black; gray shading represents the 95% confidence intervals.

around $y = 0$ for the minor *OsSOC1* variant, corresponding to flowering-time homeostasis). We hypothesize that the minor *OsSOC1* allele may have been selected by farmers to confer stability in flowering time, despite sacrificing adaptability to the local climate.

Genetic variation in *OsRGA1*, the α subunit of the rice heterotrimeric G protein, is associated with a gradient in potential evapotranspiration

PET is defined as a measure of the ability of the atmosphere to remove water through evapotranspiration given unlimited

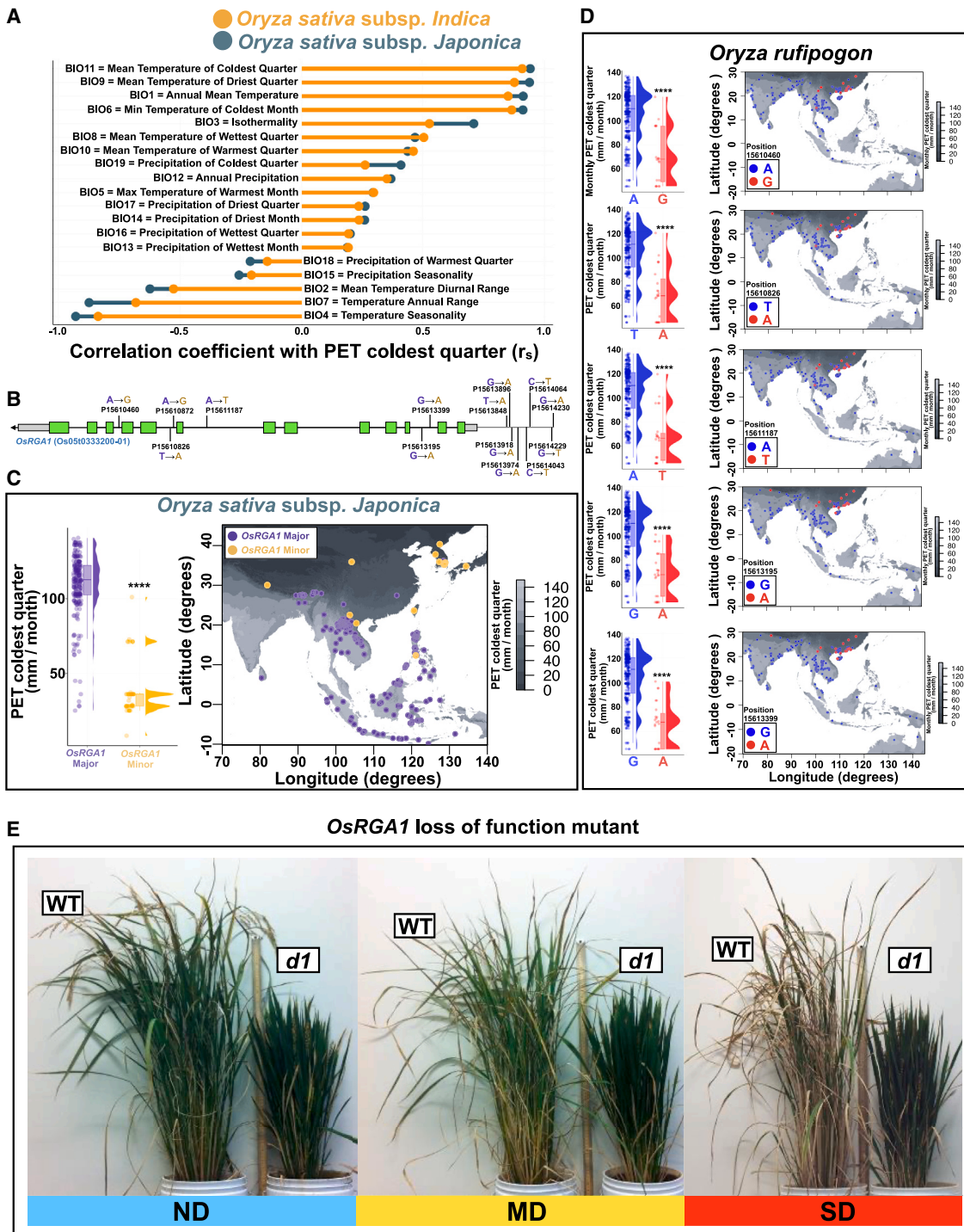


Figure 3. The haplotype distribution of SNPs in *OsRGA1* is significantly associated with the mean monthly potential evapotranspiration during the coldest quarter of the year that is typical of the local environment.

(A) The mean monthly potential evapotranspiration (PET) during the coldest quarter (“PET coldest quarter”) is co-associated with other climate variables. For example, areas with higher PET during the coldest quarter of the year are typically warmer areas with higher precipitation regimes. **(B)** We identified in Japonica landraces an allele consisting of six covarying intronic SNPs and eight upstream SNPs in *OsRGA1* (*Os05g0333200*). **(C)** Major and minor alleles of *OsRGA1* are associated with the mean monthly PET during the coldest quarter. The map of South-East Asia shows the geographic distribution of the major and minor haplotype variants of *OsRGA1*. The grayscale gradient illustrates the cline in mean monthly PET during the coldest quarter. Purple dots and distributions represent landraces harboring the major allele of *OsRGA1*. Orange dots represent landraces harboring the minor allele of *OsRGA1*.

(legend continued on next page)

moisture (Thorntwaite, 1948; Hargreaves and Samani, 1982; Penman and Keen, 1997). Therefore, PET provides an estimate of the amount of water use required for crop growth and can be used to help determine the appropriate amount of water required to optimize productivity of different varieties in a given location. We extracted the mean monthly PET of the coldest quarter (henceforth also referred to as “coldest quarter PET”) from the ENVIREM datasets (Title and Bemmels, 2018) for the local environments of rice landraces used in this study. Using bioclimatic variables derived from monthly precipitation and temperature records (Karger et al., 2017) that we collated in OryzaCLIM, we determined that coldest quarter PET was co-associated with other temperature variables for both Japonica and Indica landraces (Figure 3A). For example, areas with higher PET during the coldest quarter of the year are typically warmer areas with higher precipitation regimes (Figure 3A).

Heterotrimeric G proteins are signal transduction complexes that consist of $G\alpha$, $G\beta$, and $G\gamma$ subunits. In the classical model, upon activation of an associated G protein-coupled receptor, the $G\alpha$ subunit exchanges guanosine diphosphate (GDP) for guanosine triphosphate (GTP), resulting in dissociation from the $G\beta\gamma$ dimer. Both $G\alpha$ and $G\beta\gamma$ interact with intracellular effectors to evoke downstream signaling cascades. The system is returned to the inactive state when the intrinsic GTPase activity of $G\alpha$ hydrolyzes GTP to GDP, thereby restoring the affinity of $G\alpha$ for $G\beta\gamma$ and resulting in an inactive heterotrimeric complex (McCudden et al., 2005). The rice genome encodes one canonical $G\alpha$ (*OsRGA1*), one $G\beta$ (*OsRGB1*), and five $G\gamma$ (*OsRGG1*, *OsRGG2*, *OsGS3*, *OsDEP1*, and *OsGGC2*) subunits (Ueguchi-Tanaka et al., 2000; Utsunomiya et al., 2011). G protein subunits have been proposed to play a major role in regulating agronomic traits and stress responses (Botella, 2012; Cui et al., 2020). Our previous work specifically implicated the rice $G\alpha$ subunit, *OsRGA1*, in a number of agronomically relevant traits, including plant architecture, drought sensitivity, light-use efficiency, and mesophyll conductance (Ferrero-Serrano and Assmann, 2016; Ferrero-Serrano et al., 2018; Zait et al., 2021).

We therefore used Oryza GenoCLIM to explore possible associations between previously uncharacterized natural variation in *OsRGA1* and the local environment of rice landraces. In Japonica landraces, we identified a correlation between a haplotype consisting of six covarying intronic SNPs and eight upstream SNPs in *OsRGA1* (*Os05g0333200*; Figure 3B) and PET during the coldest quarter (Wilcoxon test, $p < 0.0001$; Figure 3C). The less frequent allele is typically associated with locations with lower PET, whereas the more frequent allele is typically found in areas with higher PET during the coldest quarter (Figure 3C).

To ascertain the ancestral origin of this $G\beta$ by E association that we found in cultivated rice landraces in a wild relative, we identified

the genetic variation present in 446 imputed sequences of *O. rufipogon* with known geographic origins using OryzaGenome 2.1 (Huang et al., 2012; Kajiya-Kanegae et al., 2021). We determined that five of the six intronic SNPs in *OsRGA1* that were associated with PET in Japonica landraces were also present in *O. rufipogon*, although not in strict covariation. We extracted the mean monthly PET of the coldest quarter from the ENVIREM datasets (Title and Bemmels, 2018) of these 446 wild rice lines and confirmed a similar pattern of association between natural genetic variation in *OsRGA1* and PET. Namely, *O. rufipogon* varieties that harbor these minor variants in *OsRGA1* are native to areas that experience lower PET. Conversely, *O. rufipogon* lines with the major variants experience higher PET (Wilcoxon test, $p < 0.0001$; Figure 3D). Our findings that genetic variation in *RGA1* is associated with a gradient in coldest quarter PET across the local environment in a wild rice relative and that both genetic variation and its association with the same environmental variable are conserved in rice landraces support the hypothesis that these natural variants in *OsRGA1* are adaptive.

In the distribution range of the georeferenced landraces studied here, areas with lower PET typically experience lower temperatures and lower precipitation regimes. We therefore hypothesized that landraces grown in climates with lower PET during the coldest quarter (and lower precipitation; Figure 3A) should have been selected for drought tolerance. To evaluate this possibility, we used the naturally occurring *d1* mutant available in the Taichung 65 (T65) Japonica cultivar, which has a 2-bp deletion in *OsRGA1* that results in a protein null allele (Oki et al., 2009). *d1* and wild-type rice plants were well watered for 60 days post germination, after which the soil was maintained at a relative water content of 100% (no drought [ND]), 45% (moderate drought [MD]), or 35% (severe drought [SD]). The dramatic drought-tolerant phenotype of *d1* is illustrated in Figure 3E. In the absence of drought (ND), both genotypes exhibited similar photosynthetic rates. However, under MD and SD, *d1* photosynthesis exceeded that of the wild type (Supplemental Figure 2).

A stop codon polymorphism in *OsGS3*, a rice G protein γ subunit, shows an association with a potential evapotranspiration gradient and interacts with *OsRGA1* to regulate vegetative and reproductive traits

Given our findings on *OsRGA1*, we next used Oryza GenoCLIM to explore the relationship between genetic variation in other G protein subunits and climate variables. We did not identify strong patterns of interaction with the environment in variants of the single rice $G\beta$ subunit gene, *OsRGB1* (*Os03g0669200*). However, we revealed a strong association between a polymorphism that introduces a premature stop codon in *OsGS3* (*Os03g0407400*), a $G\gamma$ subunit of the rice heterotrimeric G protein (Figure 4A), and the same gradient in mean PET during the coldest quarter

(D) Genetic variation in 446 imputed sequences of *O. rufipogon*. Five of the six intronic SNPs identified in *OsRGA1* in Japonica landraces (positions 15 610 460, 15 610 826, 15 611 187, 15 613 195, 15 613 399) are also associated with mean monthly PET during the coldest quarter of the year in this wild rice species. Blue dots and distributions represent landraces with the major allele of *OsRGA1*. Red dots represent landraces with the minor allele of *OsRGA1*. The same colors depict the haplotype distribution on the map of South-East Asia with a grayscale gradient that represents the cline in this drought-related variant.

(E) Confirmation of the drought tolerance of the *d1* mutant available in the Japonica cultivar Taichung 65 (T65) (see Supplemental Figure 2). In (A), r_s represents the Spearman rank correlation coefficient. In (B) and (C), $***p < 0.0001$; non-parametric Wilcoxon test.

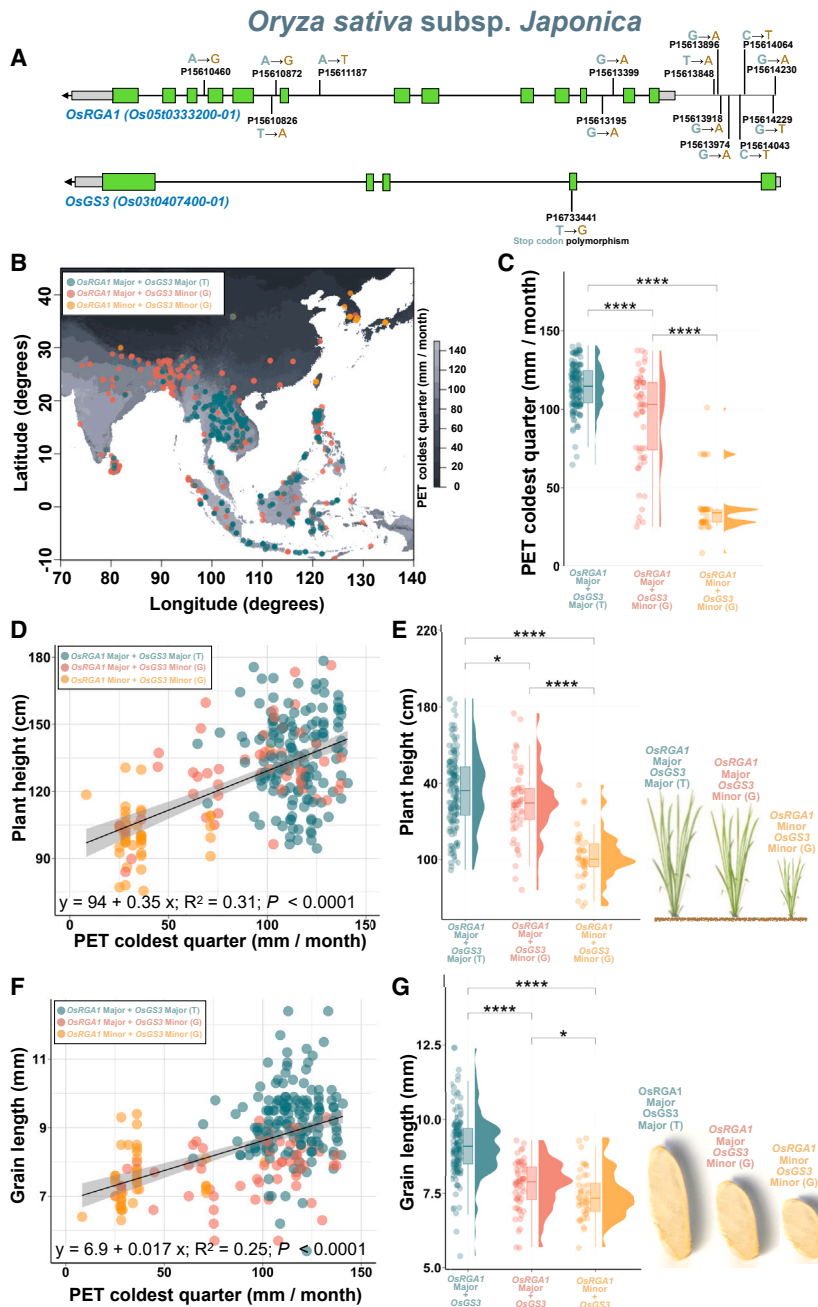


Figure 4. Haplotype distribution of *OsRGA1* and a SNP that introduces a stop codon into *OsGS3* in Japonica landraces are significantly associated with mean monthly potential evapotranspiration during the coldest quarter of the year and with natural variation in plant height and seed length.

(A) We identified in Japonica landraces an allele consisting of six covarying intronic SNPs and eight upstream SNPs in *OsRGA1* (*Os05g0333200*) and a polymorphism (G to T) that introduces a premature stop codon into *OsGS3* (*Os03g0407400*).

(B) The map of South-East Asia shows the geographic distribution of the three *OsRGA1*-*OsGS3* allelic combinations that are present with allele frequency for both genes >0.5 in Japonica landraces. The grayscale gradient illustrates the cline in potential evapotranspiration (PET) during the coldest quarter.

(C) Raincloud plots illustrate significantly different probability densities of the mean monthly PET during the coldest quarter for the three *OsRGA1*-*OsGS3* allelic combinations.

(D and E) There is a significant association between the mean monthly PET during the coldest quarter and plant height **(D)**. Allelic variation in *OsRGA1* determines the strength of this association and is strongly associated with plant height, as shown in **(E)**, consistent with the well-reported dwarf phenotype of *OsRGA1* loss-of-function mutants (Oki et al., 2009; see Supplemental Figure 2).

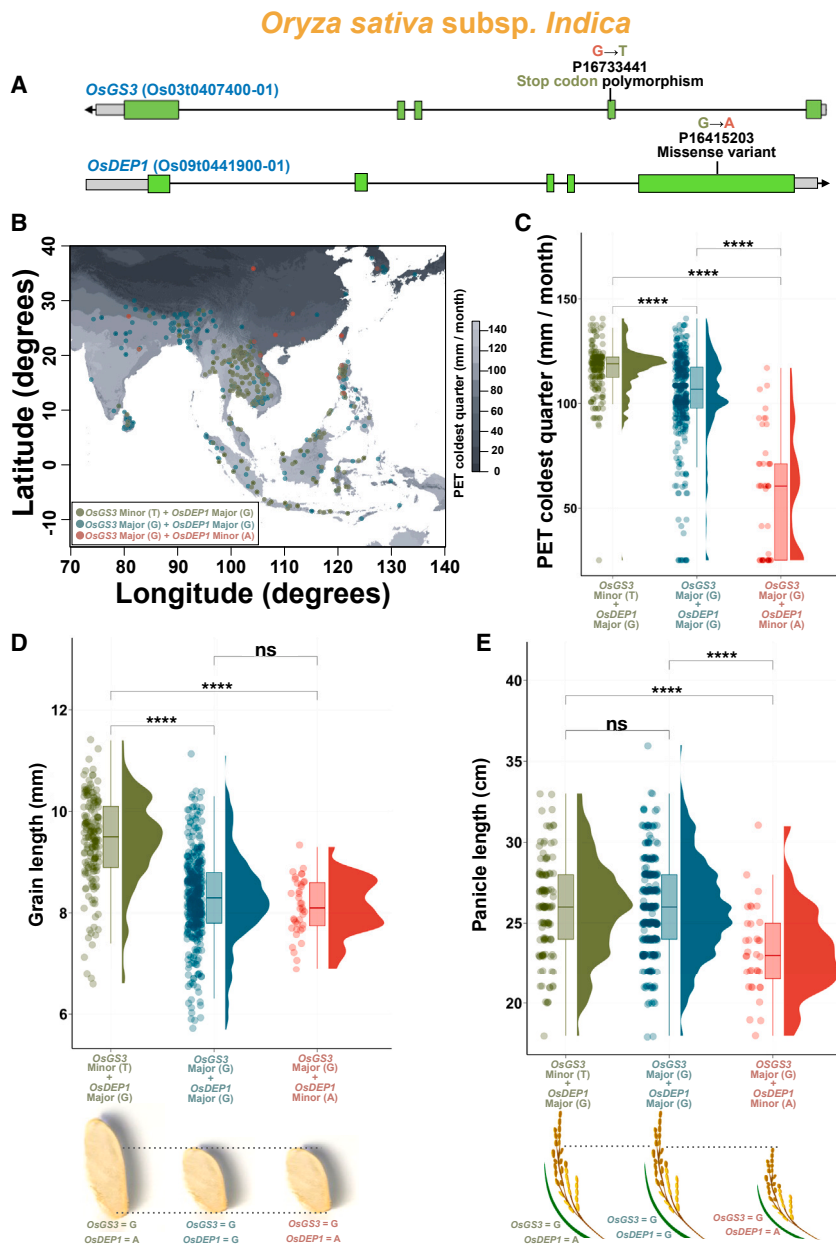
(F and G) There is also a significant association between the mean monthly PET during the coldest quarter of the year and grain length **(F)**. Allelic variation in both *OsRGA1* and *OsGS3* determines the strength of this association, and minor variants of both genes are strongly associated with shorter grains, as shown in **(G)**, consistent with the well-reported grain length phenotypes of *OsRGA1* and *OsGS3* mutants (Fan et al., 2006; see Supplemental Figure 3).

Pairwise non-parametric Wilcoxon tests were performed to assess differences between alleles. *** $p < 0.0001$.

that we identified for *OsRGA1* (Figure 4B and 4C). Interestingly, within the sequenced Japonica population, the full-length *OsGS3* allele (G) is the minor allele, whereas the allele containing the premature stop codon (T) is the major allele (Figure 4A). We used OryzaGenome 2.1 (Kajiyama-Kanegae et al., 2021) to explore genetic variation in *GS3* present in the 446 imputed sequences of *O. rufipogon* with known geographic origins (Huang et al., 2012). However, the position of *GS3* in *O. rufipogon* coincides with a region of low coverage for which no information is available, so we were unable to further investigate the presence of *GS3* SNPs in this wild rice species.

We revealed a significant association between landrace height of Japonica varieties and mean monthly PET during the coldest

quarter of the year ($R^2 = 0.31$; Figure 4D). We next found that shorter plants, which are typically found in areas with lower PET, are also more likely to possess both the minor *OsRGA1* allele and the minor (full-length) *OsGS3* allele (Wilcoxon test, $p < 0.0001$; Figure 4E). By contrast, taller plants from areas with higher evapotranspiration regimes typically harbor the major alleles of both *OsRGA1* and *OsGS3* (Wilcoxon test, $p < 0.0001$; Figure 4E). The *OsGS3* major allele, which encodes a premature stop codon, has previously been named *GS3-3* (Mao et al., 2010); here we name it *OsGS3-3* for consistency. Landrace varieties from intermediate evapotranspiration regimes typically harbor the minor *OsGS3* allele in the major *OsRGA1* allele background (Wilcoxon test, $p < 0.0001$; Figure 4C). Although plant height was significantly shorter in landrace varieties with the minor *OsGS3* allele and the major *OsRGA1* allele than in those with the major *OsRGA1* allele and the *OsGS3-3* allele (Wilcoxon test, $p < 0.05$), the average height



associated with the minor *OsRGA1* allele suggests that *OsRGA1*, not *OsGS3*, is the primary regulator of variation in plant height in a G protein-mediated process across a PET gradient.

Using a publicly available dataset of agronomic traits that includes this landrace collection (RFGB 2.0; Wang et al., 2020), we also identified a significant association between seed length of landrace varieties and coldest quarter PET ($R^2 = 0.25$; Figure 4F). Shorter grains are typical of landraces grown in low PET (drier, colder, and less isothermal areas; Figure 4F), and these varieties are more likely to harbor both the minor *OsRGA1* allele and the minor *OsGS3* (full-length) allele (Figure 4G). Landraces with longer grains, grown in warmer, wetter, and less seasonal areas, typically harbor both the major *OsRGA1* allele and the major *OsGS3* allele. Landrace varieties from areas with intermediate PET typically harbor the minor

Figure 5. Haplotype distributions of *OsDEP1* and *OsGS3* variants in Indica landraces are significantly associated with the mean monthly potential evapotranspiration (PET) during the coldest quarter of the year and with natural variation in seed and panicle length.

(A) We identified in Indica landraces a stop codon-causing (G to T) SNP in *OsGS3* and a missense variant in *OsDEP1*.

(B) The map of South-East Asia shows the geographic distribution of the major and minor variants of different *OsGS3*-*OsDEP1* allelic combinations. The grayscale gradient illustrates the gradient in mean monthly PET during the coldest quarter (“PET coldest quarter”).

(C) Raincloud plots illustrating the association of the major and minor alleles of *OsGS3* in the presence/absence of the minor allele of *OsDEP1* with PET coldest quarter. Both (B) and (C) illustrate the association of the full-length (major; G) *OsGS3* allele and the minor *OsDEP1* allele with lower-PET regions.

(D) Raincloud plot illustrates the association of the *OsGS3* major (G) vs. minor (T) variants with grain length and the lack of association of the *OsDEP1* major vs. minor variants with grain length.

(E) Raincloud plot illustrates the association of the *OsDEP1* major vs. minor variants with panicle length and the lack of association of *OsGS3* major vs. minor variants with panicle length.

Pairwise non-parametric Wilcoxon tests were performed to assess differences between alleles. *** $p < 0.0001$; ns, not significant.

OsGS3 allele in the major *OsRGA1* allele background. Average seed length is significantly shorter in landraces with the minor *OsRGA1* allele and minor *OsGS3* allele than in those with the major *OsRGA1* allele and the minor *OsGS3* allele (Wilcoxon test, $p < 0.05$). Nonetheless, the magnitude of the change in average seed length associated with the introduction of the minor *OsGS3* allele suggests that the G γ subunit (*OsGS3*) and not the G α subunit

(*OsRGA1*) is the primary regulator of variation in seed length in this G protein mechanism across a PET gradient, notwithstanding an additional contribution by *OsRGA1* (Figure 4G).

Genetic variations in the *OsGS3* and *OsDEP1* G γ subunits interact to determine seed and panicle length, but not plant height, across a potential evapotranspiration gradient

In the continued evaluation of associations between natural variation in rice G proteins and PET, we examined another G γ subunit in Indica varieties. A single non-synonymous variant in *OsDEP1* (Figure 5A) was found in association with mean monthly PET during the coldest quarter, the same environmental parameter that was associated with *OsRGA1* and *OsGS3* variants in Japonica landraces. We found that the *OsDEP1* minor allele occurred only in combination with the

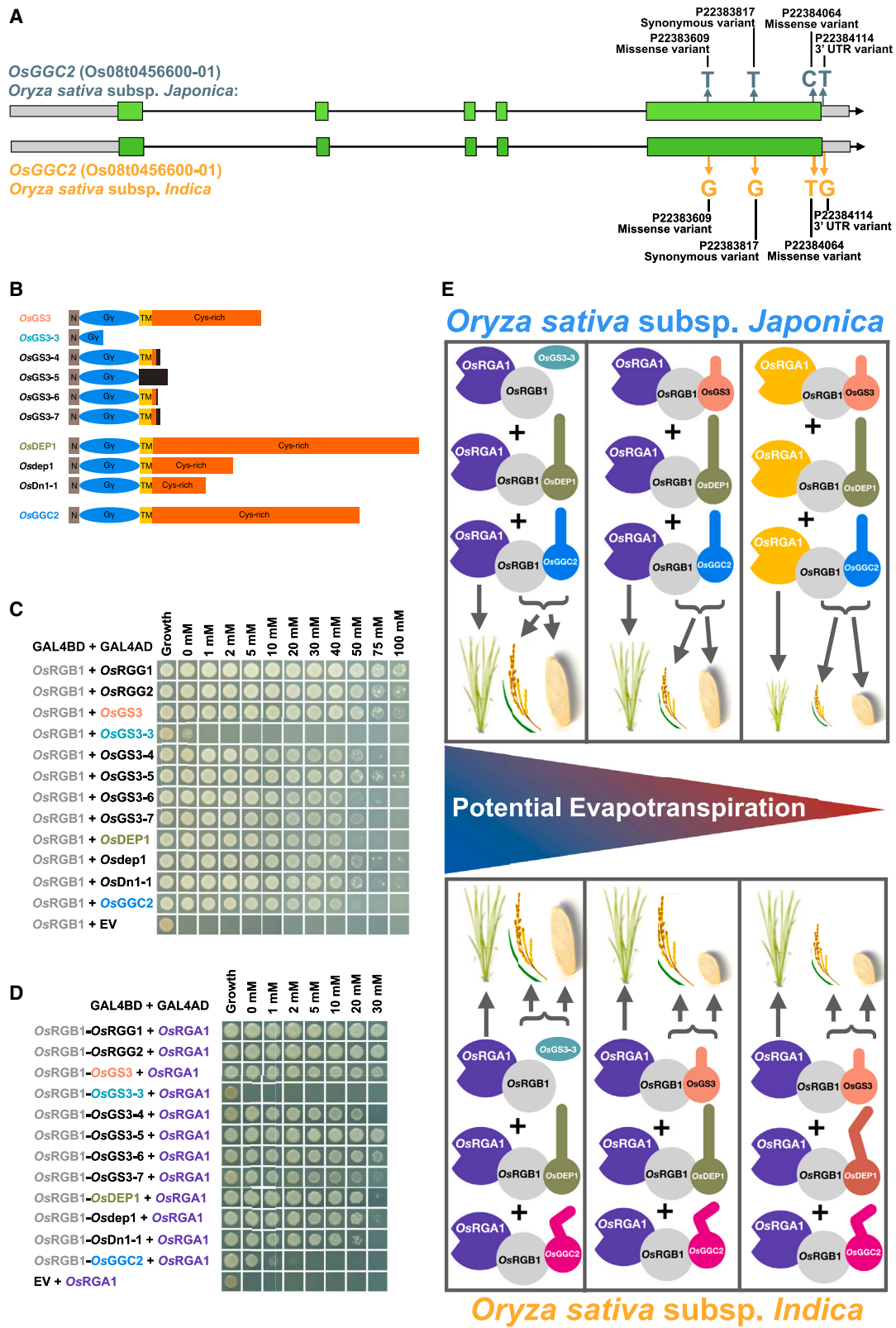


Figure 6. Genetic variation in heterotrimeric G proteins is associated with a gradient in mean monthly potential evapotranspiration during the coldest quarter of the year, and the interplay of vegetative and reproductive traits.

(A) We uncover a set of three covarying variants in the last exon and one in the 3' UTR of *OsGGC2*, with one allele typical of Japonica and the other typical of Indica varieties, that may affect the equilibrium of signaling by other G $\beta\gamma$ dimers.

(legend continued on next page)

OsGS3 major allele (which, in contrast to Japonica, is “G,” or the full-length OsGS3 allele, in the Indica population), and landraces with the *OsDEP1* minor allele and full-length OsGS3 combination are typically grown in areas with low PET (Wilcoxon test, $p < 0.0001$; **Figure 5B** and **5C**). As expected, the long-grain OsGS3-3 (non-full-length) allele (“T”) retained its association with the long-grain phenotype in Indica varieties (Wilcoxon test, $p < 0.0001$; **Figure 5D**). Variation in *OsDEP1* was found only in varieties with a full-length OsGS3 allele and was not found in association with variation in grain length in the absence of variation in OsGS3 (Wilcoxon test, $p > 0.05$; **Figure 5D**). This suggests that grain length is regulated by natural variation in OsGS3 and not *OsDEP1*. Notably, the minor allele of *OsRGA1* (**Figures 3B** and **4A**) was not present in any of the 658 Indica landraces, meaning that no genetic interaction was possible between *OsRGA1* and OsGS3 or *OsDEP1* in this Indica population.

When we evaluated the association of OsGS3 and *OsDEP1* with panicle length, using data obtained from a publicly available dataset that includes this landrace collection (RFGB 2.0; [Wang et al., 2020](#)), we found that Indica varieties with the minor *OsDEP1* allele had shorter panicles than those with the major allele, regardless of the presence of OsGS3 variation in this major *OsDEP1* allele background (Wilcoxon test, $p < 0.0001$; **Figure 5E**). This result suggests that panicle length is regulated by natural variation in *OsDEP1* and not OsGS3.

To support the observation that variants in the $G\alpha$ subunit, *OsRGA1*, and not the $G\gamma$ subunits regulate plant height, as observed in *OsRGA1* and OsGS3 Japonica lines (**Figure 4E**), we explored existing variation in plant height across different OsGS3-*OsDEP1* allelic combinations in these Indica landraces. Because all Indica landraces harbor the major *OsRGA1* allele, the lack of association between plant height and any combination of OsGS3-*OsDEP1* alleles (Wilcoxon test, $p > 0.05$; [Supplemental Figure 3](#)) confirms that natural variation in these $G\gamma$ subunits does not influence plant height in Indica landraces.

Agronomic traits regulated by natural variation in G proteins that affects the nature of their protein–protein interactions

As described above, we used Oryza CLIMtools to reveal associations of G protein natural variants in Indica and Japonica landraces with the local environment and with adaptive agronomic traits. Our observation that natural variation in *OsDEP1* and not

OsGS3 regulates panicle length in Indica, whereas variation in *OsRGA1* and OsGS3 does so in Japonica (Wilcoxon test, $p < 0.0001$; [Supplemental Figure 4](#)), may be explained by (1) the absence of the *OsRGA1* minor allele in Indica and (2) the different versions of a third $G\gamma$ subunit, OsGCC2, that were observed in Indica and Japonica. In OsGCC2, a set of three variants in the last exon and one in the 3' untranslated region (UTR) covary, defining one allele that is categorically found in all Japonica landraces in CLIMtools and another that is categorically found in Indica landraces in CLIMtools (**Figure 6A**). Given that rice $G\gamma$ subunits are known to function both additively and antagonistically ([Sun et al., 2018](#)), a difference in OsGCC2 function may shift the equilibrium of signaling from other $G\beta\gamma$ dimers and thereby alter the genetic interactions between subunits.

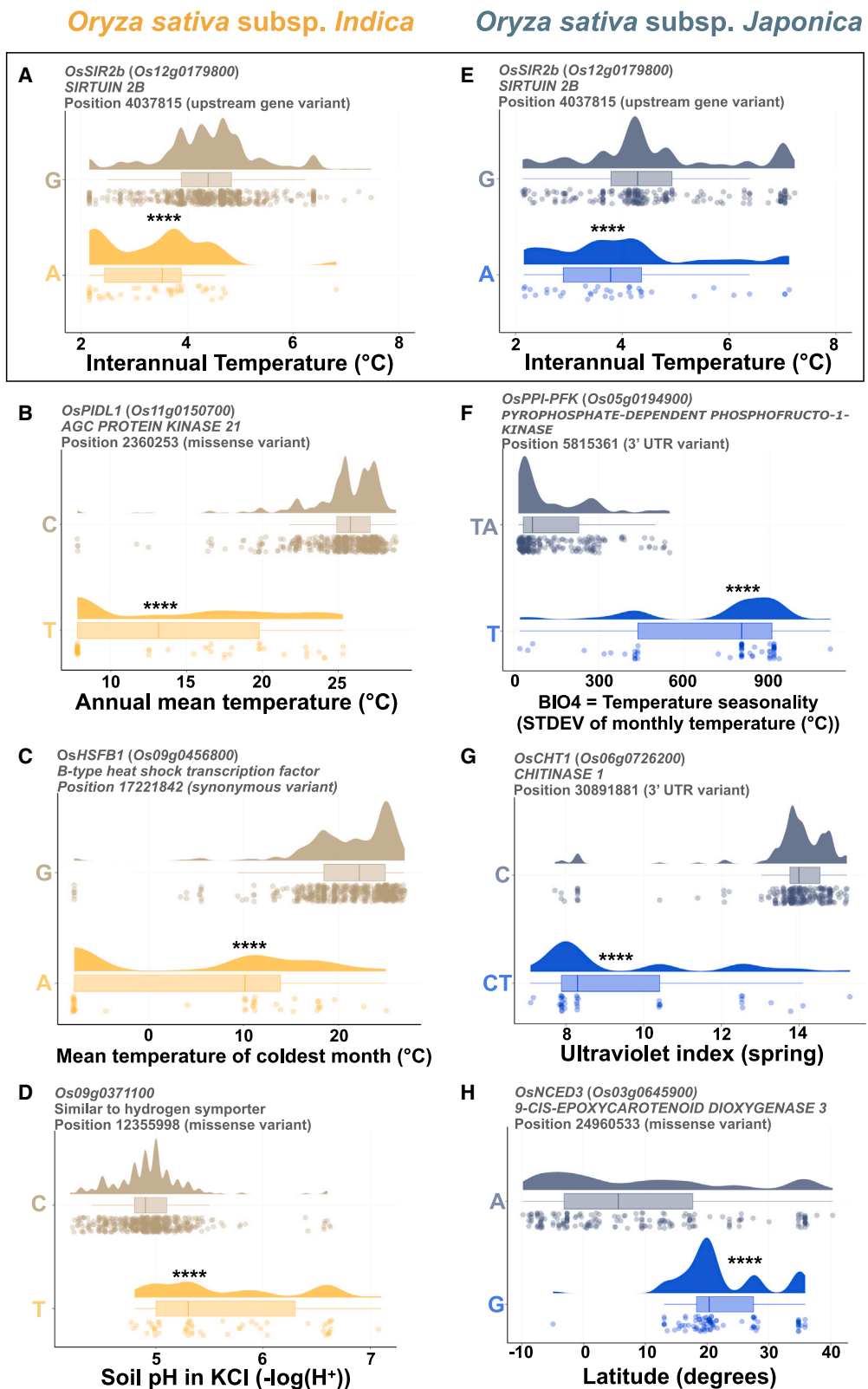
We have previously shown that a C-terminal truncation of the *Arabidopsis* ortholog of OsGS3, *AtAGG3*, which retains only part of the $G\gamma$ domain (residues 1–78), loses interaction with the *Arabidopsis* $G\beta$ subunit ([Chakravorty et al., 2011](#)). We therefore hypothesized that the similarly truncated protein encoded by the Japonica major allele/Indica minor allele (T) of OsGS3, OsGS3-3 (**Figure 6B**), would also not bind the rice $G\beta$ subunit. Using a yeast two-hybrid assay of protein–protein interaction, we observe that the protein encoded by the OsGS3-3 allele indeed shows severely impaired interaction with *OsRGB1*, as evidenced by weak yeast growth that occurs only in the absence of 3-aminotriazole (3-AT); **Figure 6C**). By contrast, all full-length $G\gamma$ subunits, corresponding to the Japonica Taichung 65 sequences of *OsRGG1*, *OsRGG2*, OsGS3, *OsDEP1*, and OsGCC2, strongly bound *OsRGB1*, as assessed by growth on a semi-quantitative 3-AT concentration curve (**Figure 6C**). The previously identified truncations resulting from indels in OsGS3 or *OsDEP1* that retain a full $G\gamma$ domain (**Figure 6B**), namely OsGS3-4 ([Mao et al., 2010](#)), OsGS3-5, OsGS3-6, OsGS3-7 ([Takano-Kai et al., 2013](#)), *Osdep1* ([Huang et al., 2009](#)), and *OsDn1-1* ([Taguchi-Shiobara et al., 2011](#); alignments in [Supplemental Figure 5A](#) and [5B](#)), also bound *OsRGB1* with similar or increased strength compared with the corresponding wild-type subunits (**Figure 6C**). As expected, no $G\gamma$ subunits displayed any growth on interaction-selective media in combination with the empty vector control (negative control; [Supplemental Figure 5C](#)). We also used a yeast three-hybrid approach to assess the interactions of different $G\beta\gamma$ dimers with $G\alpha$ subunits. Consistent with our yeast two-hybrid data, the truncated OsGS3-3 protein did not allow heterotrimer

(B) Domain schematic of rice type C $G\gamma$ subunits, indicating known truncations. N, N-terminal sequence; $G\gamma$, $G\gamma$ -like domain; TM, putative transmembrane domain; Cys-rich, C-terminal Cys-rich domain. The dark-gray boxes correspond to out-of-frame translated regions. See [Supplemental Figure 5A](#) and [5B](#) for multiple alignments of protein sequences.

(C) Yeast two-hybrid assays between $G\beta$ (*OsRGB1*) and $G\gamma$ show the lack of interaction between *OsRGB1* and OsGS3-3 and the positive interactions between *OsRGB1* and all other $G\gamma$ subunits.

(D) Yeast three-hybrid assays between $G\beta\gamma$ dimers and the canonical $G\alpha$, *OsRGA1*, show that all *OsRGG1*, *OsRGG2*, OsGS3, *OsDEP1*, and OsGCC2 proteins encoded by $G\gamma$ alleles were able to complex with *OsRGB1* and *OsRGA1* via *OsRGB1*, with the exception of OsGS3-3. Assays in **(C)** and **(D)** were spotted on SC-Trp-Leu medium as a growth control and on SC-Trp-Leu-Met-His medium with the indicated concentrations of 3-amino-1,2,4-triazole (3-AT) to assess interaction strength. 3-AT is a competitive inhibitor of the *HIS3* reporter gene of the yeast two-/three-hybrid system and therefore enables semi-quantitative assessment of interaction strength, with growth at higher 3-AT concentrations indicating a stronger interaction.

(E) Illustration summarizing our hypothesis for how agronomic traits are affected by alternative combinations of different heterotrimeric G protein variants associated with mean monthly potential evapotranspiration during the coldest quarter of the year. Color coding for $G\gamma$ alleles is as in **(B)**–**(D)**. Color coding: *OsRGA1*, purple = major allele and yellow = minor allele; *OsRGB1*, gray; OsGS3, salmon = full-length allele and turquoise = OsGS3-3 truncated allele; *OsDEP1*, olive green = major allele and orange-red = minor allele; OsGCC2, light blue = Japonica allele and pink = Indica allele. See [discussion](#) for details.



(legend on next page)

formation with *OsRGA1* (Figure 6D). The full-length Taichung 65 G_γ subunits all allowed heterotrimer formation with *OsRGA1* (Figure 6D). The variant G_γ proteins *OsGS3-4*, *OsGS3-5*, *OsGS3-6*, *OsGS3-7*, *Osdep1*, and *OsDn1-1* also allowed heterotrimer formation (Figure 6D). These results indicate that the *OsGS3-3* allele likely acts as a functional null owing to its inability to complex with other G protein subunits. By contrast, G_γ truncations that can bind G_β may act as dominant negatives or may sequester G_α and G_β subunits, as we have previously shown that the Cys-rich tail of the *Arabidopsis* ortholog of *OsGS3*, *AtAGG3*, is required for G_γ function (Chakravorty et al., 2011). We did not examine interactions of the proteins encoded by the *OsDEP1* minor allele (*OsDEP1*^{C261Y}) or the *OsGGC2* Indica allele (*OsGGC2*^{L169W R321C}) with *OsRGB1* or with *OsRGA1* when contained within the $\text{G}_\beta\text{G}_\gamma$ dimer; the changes encoded within these G_γ protein variants occur in the Cys-rich tail, a region of type C G_γ subunits that, while important (Chakravorty et al., 2011), does not contribute to binding of other heterotrimeric G protein subunits (Chakravorty et al., 2011), and the tail is proposed to reside in the apoplast (Wolfenstetter et al., 2015).

In Figure 6E, we synthesize all our G protein-related findings to propose a molecular mechanism by which natural variants in rice G proteins regulate signaling, with phenotypic consequences (see discussion).

CLIMtools enables broad exploration of the genetic basis of local adaptation in rice

Above, we demonstrated the utility of Oryza CLIMtools in revealing adaptive associations between phenotypes and environmental variables codified in OryzaCLIM. We used these tools to focus on the agronomic roles of variation in heterotrimeric G proteins. It is unavoidable that our dataset may be missing alleles that are only present in geographic locations for which georeferenced landrace data are not available. However, as shown in Figure 7, Oryza CLIMtools can be used broadly to investigate many putative mechanisms for the potential genetic bases of adaptation to diverse climate variables, including various temperature measures (Wilcoxon test, $p < 0.0001$; Figure 7A–7C, 7E, and 7F), soil quality (Wilcoxon test, $p < 0.0001$; Figure 7D), illumination conditions (Wilcoxon test, $p < 0.0001$; Figure 7G), and aggregating variables such as latitude (Figure 7H).

DISCUSSION

Rice is the staple food for more than half of the world's population and the main source of calorie intake in emerging and developing economies (Seck et al., 2012); any reduction in global production will have important implications for food security worldwide (Godfray et al., 2010). A major challenge is thus to feed the burgeoning human population while mitigating crop losses incurred as a result of climate change.

There is a mismatch between the current distributions of crop varieties and climate suitability for their production. Breeding programs that introduce genetic diversity from local landraces can help to address this challenge (Hoisington et al., 1999; Fu and Somers, 2009; Zhang et al., 2017; Renard and Tilman, 2019) but will benefit from taking environmental factors into account. To date, no comprehensive resource has been available for investigating the relationship between genetic and environmental variation that exists in the local environments where rice landraces are grown. With this in mind, we created OryzaCLIM (https://gramene.org/CLIMtools/oryza_v1.0/OryzaCLIM/), an intuitive online resource for exploration of 413 geoenvironmental variables that define local environmental conditions at the collection sites of 658 Indica and 283 Japonica sequenced landraces (Figure 1).

We then evaluated several significant (FDR < 0.01) climate–gene associations identified using Oryza CLIMtools to illustrate the utility of our resources and show how these associations can be validated to demonstrate causality.

Flowering time and temperature

Average global temperatures are predicted to increase by 1.5°C between 2030 and 2052 (Delmotte et al., 2018). These rising temperatures pose a significant threat to rice production (Zhao et al., 2016), and flowering is the developmental stage most sensitive to heat stress (Matsui et al., 2001; Jagadish et al., 2010). Indeed, supraoptimal temperatures increase spikelet sterility and critically reduce rice yield (Shrestha et al., 2022).

Many species in natural settings demonstrate shifts in flowering time associated with ongoing climate change (Fitter and Fitter, 2002). In the case of rice, modern high-yielding cultivars are grown in many areas of the world that differ enormously in their environmental conditions. The flowering time of these modern cultivars is not optimized for all local environments. By contrast, local landraces are cultivated varieties that have evolved as a result of both natural and artificial selection (Casañas et al., 2017) and are therefore amenable to mining for adaptations of flowering time to the local environment.

Temperature is a key environmental factor patterning contemporary rice genomic diversity (Gutaker et al., 2020). Indica and Japonica landrace varieties show considerable phenotypic variability in flowering time (Supplemental Figure 6A), and here we show that flowering time in both Indica and Japonica landraces is significantly associated with the minimum temperature of the coldest month in their local environment (Figure 2B and 2D). Rice is a facultative short-day plant. Many landraces in tropical and subtropical regions have mild photoperiod sensitivity that inhibits flowering under long days and promotes flowering under short days, maximizing the time for vegetative growth before flowering (Zong et al., 2021). At the same

Figure 7. Examples of genotype-by-environment associations found using Oryza CLIMtools.

(A–D) Example associations for Indica landraces between (A) an upstream gene variant in *OsS/R2b* and interannual temperature, (B) a missense variant in *OsPID1* and annual mean temperature, (C) a synonymous variant in *OsHSFB1* and mean temperature of the coldest month, and (D) a missense variant in *Os09g0371100* and soil pH.

(E–H) In Japonica landraces, we found an association between (E) the same upstream variant identified in Indica landraces in *OsS/R2b* and the same climate parameter, interannual temperature, (F) a 3' UTR indel variant in *OsPPI-PFK* and temperature seasonality, (G) a 3' UTR indel variant in *OsCHT1* and UV index during the spring season, and (H) a missense variant in *OsNCED3* and latitude.

time, suboptimal temperatures negatively affect survival and yield (Zhang et al., 2014), and varieties from areas with suboptimal temperatures during the cold season sacrifice vegetative growth but ensure early flowering and seed production before the onset of low temperatures concurrent with shorter photoperiods. Here, we described the relationship between flowering time and temperature in the local environment for a fully sequenced rice population. The introduction of flowering-time stability, as provided by the minor allele of *OsSOC1* (Figure 2D and 2E), may provide an agronomically desirable trait whose benefits outweigh its climate incompatibility.

Our dataset covers a vast geographic range of 6730 km in longitude and 3388 km in latitude (Figure 1). However, it does not provide comprehensive, geographically dense coverage in areas such as China and other higher-latitude regions, owing to a lack of georeferenced landrace data from these regions. Previous studies that have focused on these regions have identified *OsHD1* and *OsGhd7* (Zhang et al., 2015; Han et al., 2016) as major regulators of flowering time in response to photoperiod. In our datasets, natural variants in these photoperiod-responsive genes in significant association with latitude were also identified ($p < 0.0001$; Supplemental Document 1), confirming previous reports on datasets from high-latitude regions (Zhang et al., 2015; Han et al., 2016).

In addition to photoperiod, temperature is also a major regulator of flowering-time transition, and we identified an adaptive association between an allele of *OsHD2* and the minimum temperature of the coldest month (Figure 2B). *OsHD2* has been identified as a flowering-time quantitative trait locus (QTL) that is important for temperature regulation of photoinduction (Nakagawa et al., 2005). The *Arabidopsis* ortholog of *OsHD2*, *AtPRR7*, is a key component of the temperature compensation mechanism that maintains a constant circadian rhythm under changing temperatures (Salomé et al., 2010). Consistent with our findings, previous work has shown that functional alleles of *OsHD2*, known to produce higher yields, are found mainly in warmer southern latitudes, whereas “weaker” and early-flowering, non-functional alleles of *OsHD2* are found in colder, northern latitudes (Koo et al., 2013; Yan et al., 2013; Li et al., 2015; Ye et al., 2018). These results are also consistent with the findings of Guo et al. (2020), who determined that varieties from areas with lower local temperatures are enriched in *OsHD2* allelic variants that are associated with temperature sensitivity of flowering time. Conversely, varieties from areas with warmer temperatures harbor *OsHD2* alleles that are associated with temperature-invariant flowering times.

Because environmental variables are often correlated with one another (Supplemental Figure 1), it is possible that other co-correlated variables also contribute to adaptation of flowering time to the local environment. Indeed, we observed that the minimum temperature of the coldest month was correlated with other temperature and precipitation seasonality variables (Supplemental Figure 7).

Given this finding, we propose that *OsHD2* is a key mediator of the adaptation of flowering time to the local environment. The feasibility of fine-tuning flowering time via genome editing of the

upstream open reading frame (ORF) of *OsHD2* has also been demonstrated (Liu et al., 2021). We can envision an approach by which the appropriate flowering time of any variety can be modulated to match local temperatures, thus creating varieties that are better adapted to their local climate and maximizing their potential yield in a given location. Oryza CLIMtools opens the door to exploring the genetic basis of flowering-time adaptation so that flowering time can be tailored to match environmental conditions in a given cultivation area.

Genetic variation in the heterotrimeric G protein $G\alpha$ subunit *OsRGA1* is associated with a gradient in potential evapotranspiration

Most modern, high-yielding rice varieties rely on a mutant *SD-1* gene, introduced during the Green Revolution, as the basis of their semi-dwarf phenotype (Hargrove and Cabanilla, 1979; Hargrove et al., 1980; Ferrero-Serrano et al., 2019). However, the *qDTY1.1* allele, a QTL for drought tolerance, has been lost in these modern varieties because of its tight linkage in repulsion with the *sd1* allele. Consequently, the widespread use of *sd1* as a source of dwarfism has both reduced the genetic diversity of this trait and resulted in modern rice cultivars that are typically drought sensitive. This illustrates one of the best documented consequences of genetic erosion in crops: the reduction in adaptability or tolerance to abiotic factors (Khoury et al., 2022).

Drought is one of the most widespread and damaging environmental stress factors (Farooq et al., 2012; Gupta et al., 2020) and affects rice, particularly as varieties are often adapted to either rain-fed or fully irrigated systems. For this reason, identification of an alternative source of dwarfism that also provides an adaptive advantage under drought could contribute to stability in global yield production. In this study, we argue that natural variants in other dwarfing genes are available that are positively associated with drought-related environments.

Following this rationale, we explored the association of naturally occurring variants in the heterotrimeric G protein $G\alpha$ subunit, *OsRGA1*, with the local environment, particularly drought-related environmental variables. Naturally occurring functional null *OsRGA1* mutants display a characteristic dwarf phenotype (Ashikari et al., 1999; Oki et al., 2009; Ferrero-Serrano and Assmann, 2016; Zait et al., 2021). Loss-of-function *OsRGA1* dwarf mutant plants show greater drought resistance than wild-type plants as a consequence of their increased water-use efficiency, increased mesophyll conductance, lower leaf temperature, and increased light-use efficiency (Ferrero-Serrano and Assmann, 2016; Ferrero-Serrano et al., 2018; Zait et al., 2021).

Using Oryza GenoCLIM (https://gramene.org/CLIMtools/oryza_v1.0/Oryza_GenoCLIM/), we identified a set of covarying SNPs in the intronic and upstream regions of *OsRGA1* (Figure 3B) that were in association with a gradient in mean monthly PET during the coldest quarter of the year. The minor allele is found in landraces collected from areas with lower PET, and the most frequent allele (major allele) is present in landraces collected from areas with higher PET (Figure 3C).

PET provides an estimate of the amount of water used for growth and can therefore be used to select drought-tolerant varieties. As

shown in [Figure 3A](#), areas with lower PET during the coldest quarter have colder but also more variable temperatures throughout the year and lower precipitation regimes. In other words, areas with lower PET are associated with more challenging and unpredictable environments ([Figure 3A](#)). We hypothesize that landraces from areas with lower PET will have improved tolerance to multiple abiotic stress factors, a trait in which G proteins play a critical role ([Wu and Urano, 2018](#); [Wang and Botella, 2022](#)). We illustrate this point by showcasing the improved drought tolerance of the *OsRGA1* natural null mutant, *d1* ([Figure 3E](#)).

The role of the minor *OsRGA1* variant in adaptation to regions with lower PET during the coldest quarter is supported by our finding that five of the six intronic *OsRGA1* variants that we found in rice landraces are conserved in the ancestral species of rice, its wild rice relative *O. rufipogon* ([Huang et al., 2012](#)), where they are also associated with a gradient in PET ([Figure 3D](#)). This finding in an ancestor of domesticated rice supports the hypothesis that natural variation in *OsRGA1* is adaptive across a PET gradient in South-East Asia.

Genetic variation in heterotrimeric G proteins is associated with a potential evapotranspiration gradient and the interplay of vegetative and reproductive traits

Previous studies have typically described the agriculturally relevant roles of individual G protein subunits and their variants in isolation ([Botella, 2012](#); [Wu et al., 2022](#); [Ferrero-Serrano and Chakravorty, 2023](#)). Here, we reveal how interaction among natural variants in the $G\alpha\beta\gamma$ complex determines agronomic traits and stress responses that contribute to fitness in the local environment. Although we did not identify variants of interest in *OsRGB1*, we found different natural variants of the $G\gamma$ subunits in association with PET, the same environmental variable associated with the *OsRGA1* variants, suggesting a genetic interaction.

$G\gamma$ proteins are divided into three distinct groups on the basis of their C-terminal domains. The rice genome encodes two shorter $G\gamma$ subunit proteins, *OsRGG1* (type A) and *OsRGG2* (type B), and three longer $G\gamma$ subunits with a Cys-rich tail, *OsDEP1*, *OsGGC2*, and *OsGS3* (type C; [Trusov et al., 2012](#)). A number of indels have been identified in *OsGS3* and *OsDEP1* ([Figure 6B](#)) that confer changes in grain shape ([Mao et al., 2010](#); [Takano-Kai et al., 2013](#)) and a dense and erect panicle morphology ([Huang et al., 2009](#); [Taguchi-Shiobara et al., 2011](#)), respectively.

In Japonica rice, the minor allele of *OsRGA1* is associated with extremely short grains, significantly shorter than those conferred by the major *OsRGA1* allele in combination with the minor (full-length) *OsGS3* allele ([Figure 4G](#)). The role of *OsRGA1* may therefore involve impairment of *OsDEP1* and *OsGGC2* signaling. Indeed, knockout of either *OsDEP1* or *OsGGC2* results in short plant, panicle, and grain phenotypes that are epistatic to *OsRGA1 d1* mutations ([Sun et al., 2018](#); [Chaya et al., 2022](#)). *OsGS3* allele frequency in Indica rice is the opposite of that seen in Japonica ([Figure 4B](#) vs. [Figure 5B](#)). In Indica landraces, the minor allele of *OsGS3*, previously named both *gs3* and *GS3-3*, is the allele that encodes a premature stop codon (T) within the $G\gamma$ domain. This allele has been found

to cause a long-grain phenotype ([Fan et al., 2006](#); [Mao et al., 2010](#)), which we now show is found in areas of higher PET ([Figure 4B](#) and [4C](#)). The *OsGS3-3* variant was introduced from Japonica ancestor(s) into the Indica gene pool ([Takano-Kai et al., 2009](#); [Mao et al., 2010](#)), which may explain why the frequency of the *OsGS3-3* allele is higher in the Japonica population than in the Indica population.

The *OsGS3-3* protein, but not other *OsGS3* variants, failed to interact with either *RGA1* ([Figure 6D](#)) or any of the rice extra-large $G\alpha$ subunits (*OsXLGs*; [Cantos et al., 2023](#)) ([Supplemental Figure 5D–5G](#)), strengthening our conclusion that the truncated *OsGS3-3* protein is non-functional. We also found that the *OsGS3-3* protein is unable to dimerize with $G\beta$ ([Figure 6C](#)); this eliminates *OsGS3-3* competition for $G\beta$ dimerization with the $G\gamma$ subunits that promote grain elongation, *OsDEP1* and *OsGGC2* ([Sun et al., 2018](#)), resulting in a long-grain phenotype. By contrast, multiple *OsGS3* mutants that result in a super short-grain phenotype ([Takano-Kai et al., 2013](#)) retain the ability to interact with *OsRGB1* (i.e., *OsGS3-4*, *OsGS3-5*, *OsGS3-6*, and *OsGS3-7*) ([Figure 6B](#) and [6C](#)), consistent with their ability to partially suppress *OsDEP1* and *OsGGC2* dimerization with $G\beta$, despite presumably not retaining full intrinsic signaling functionality of their own.

Because our observations of genetic interaction between different $G\gamma$ subunit variants are consistent with the concept of $G\gamma$ competition for dimerization with the $G\beta$ subunit, introgression of different $G\gamma$ alleles into elite varieties is likely to have unintended effects on signaling from other heterotrimeric G protein components. Such scenarios of pleiotropism and genetic interactions are not uncommon, and we envision that Oryza CLIMtools will facilitate the identification of sources of complementary genetic variation and suitable genetic backgrounds for rational breeding and genetic improvement programs. Moreover, unlike previous studies, CLIMtools provides this information in the context of environmental adaptations. As an example, we discovered that the full-length *OsGS3* allele is found in areas of lower PET—and lower temperatures—in both Japonica ([Figure 4B](#) and [4C](#)) and Indica landraces ([Figure 5B](#) and [5C](#)). Consistent with these results, our previous work identified a role for the *Arabidopsis* ortholog *AtAGG3* ([Chakravorty et al., 2011](#)) in adaptation to cold temperatures and an association of a missense (minor) variant in *AtAGG3* with colder areas in northern Eurasia ([Ferrero-Serrano and Assmann, 2019](#)).

OsDEP1, originally identified as an erect panicle QTL ([Kong et al., 2007](#); [Yan et al., 2007](#)), encodes another $G\gamma$ protein that, like *OsGS3*, is a type C $G\gamma$ subunit with a Cys-rich tail. Natural variation in *OsDEP1* regulates meristematic activity, with a previously described variant resulting in reduced length of the inflorescence internode, erect and shorter panicles, an increased number of grains per panicle, and a consequent increase in grain yield ([Huang et al., 2009](#)). This variant involves replacement of a 637-bp stretch of the middle of exon 5 with a 12-bp sequence, creating a premature stop codon and the loss of 230 residues from the C terminus ([Huang et al., 2009](#)). The variant we identify here is a missense variant that also occurs in the middle of the fifth exon ([Figure 5A](#)). As observed for *OsGS3*, variation in *OsDEP1* is also associated with coldest quarter PET ([Figure 5B](#) and [5C](#)). However, on the basis of our analysis of panicle length

in Indica landraces, we propose that natural variation in *OsDEP1*, but not *OsGS3*, is responsible for variation in this phenotype in Indica varieties. We reach this conclusion because of the association of the minor *OsDEP1* allele with shorter panicle phenotypes and the major *OsDEP1* allele with longer panicle phenotypes, independent of a full-length/truncated *OsGS3* allele (Figure 5E). Although this conclusion might be challenged by our observation of differences in panicle length in Japonica landraces associated with natural variation in *OsRGA1* and *OsGS3* (Supplemental Figure 4), we suggest that this apparent discrepancy may be due to an interaction with the *OsRGA1* allele in Japonica that is not possible in Indica, which completely lacks the *OsRGA1* variants that we describe. Alternatively, there may be a genetic interaction with the different haplotype versions of *OsGCC2* present in Indica vs. Japonica (Figure 6A).

We recently proposed a mechanism regulated by G proteins, particularly the $G\alpha$ subunit, that involves a trade-off between growth and stress tolerance that is critical for mediating adaptability (Ferrero-Serrano and Chakravorty, 2023). We hypothesize that landraces from areas with lower coldest quarter PET (typically at higher latitudes; Figure 3C) experience a “less predictable” environment (Figure 3A) and trade off their stress tolerance with a derived growth cost that is illustrated by the reduced stature associated with the minor *OsRGA1* allele (Figure 4D and 4E). This point is illustrated not only by the increased drought tolerance of the dwarf *d1* mutant but also by previous findings relating $G\alpha$ loss-of-function mutants with resistance to diverse stresses in other species (Zhang et al., 2008; Nilson and Assmann, 2010; Jangam et al., 2016; Ferrero-Serrano et al., 2018; Cui et al., 2020). We also highlight the association of natural variation in the $G\gamma$ subunit with the same environmental gradient that we found in association with *OsRGA1* variants, PET during the coldest quarter, and, in this case, also with reproductive traits that are important for maximizing yield (Figure 6E). These results highlight the potential of modulating G protein function for vegetative stress tolerance and the associated interplay between stress tolerance, growth, and yield.

In summary, we have demonstrated the utility of Oryza CLIMtools for uncovering adaptive genetic variation associated with existing natural variation in agronomic traits. The ultimate goal is to incorporate information derived from landraces into modern varieties and test them in appropriate multi-year and multi-environment trials, using appropriate guidelines (Khaipho-Burch et al., 2023), to develop better-adapted varieties that will improve food security and sustainability.

METHODS

Extraction of environmental variables

We compiled a comprehensive database of environmental data for 658 Indica and 283 Japonica georeferenced landrace varieties included in the 3K Rice Genome Project (Gutaker et al., 2020, which includes 413 geoclimatic variables describing the local environment at each collection site (Supplemental Figure 1 and Supplemental Table 1). We used the Raster package in R (Hijmans et al., 2013) to extract geospatial Raster data for

the environmental conditions prevailing at each landrace’s collection site. A detailed list of relevant literature references that describe the climate dataset from which we curated the environmental information, as well as summary statistics for each of the 413 environmental variables, can be found in Supplemental Table 2.

OryzaCLIM

We developed OryzaCLIM, a user-friendly Shiny component (Chang et al., 2015a) of Oryza CLIMtools that enables the analysis of local environmental data for georeferenced accessions (Gutaker et al., 2020) sequenced as part of the 3K Rice Genome Project (Wang et al., 2018). OryzaCLIM incorporates 413 environmental variables that have been codified to facilitate examination of the environmental conditions at the collection sites of 658 Indica and 283 Japonica georeferenced landraces. These data points are represented on an interactive world map that enables users to analyze pairwise environmental conditions for these 941 landrace varieties.

By clicking on any of the data points on the map, users can access information about the selected variety, including its curation details and the value of the chosen environmental variable.

GWA analysis

We obtained SNP and indel data from the 3K genomes (https://snp-seek.irri.org/_download; zulj/sessionid=0E0F5BCFB0EA14EBB926BEBC7B26D6E0) and converted the data from Plink format to VCF format using PLINK 2.0 (Chang et al., 2015b). We used VCFtools (Danecek et al., 2011) to subset the resulting VCFs into separate files for the 658 Indica and 283 Japonica landrace varieties that were the focus of this study. The data were filtered to select genetic variants with less than 10% missing data and a minimum allele frequency (MAF) $\geq 5\%$. After this initial filtering, imputation was performed using BEAGLE v5.4 with default parameters (Browning et al., 2018).

Rice includes two major subspecies: *Oryza sativa* ssp. *indica* and *O. sativa* ssp. *japonica*. Differences between subspecies are apparent in a number of physiological and morphological traits, genetic variation, and geographic distribution (Khush, 1997; Garris et al., 2005; Huang et al., 2012; Wang et al., 2018). Our own analysis of previously characterized agronomic traits (Wang et al., 2020) in the set of landrace varieties used in this study revealed that Indica landrace varieties typically display more culms that are longer, longer leaves that are narrower, shorter stature at the seedling stage, earlier flowering, more panicles, and longer grain than Japonica varieties (Supplemental Figure 6). Given such marked subspecies differences, we performed GWA analysis separately for the Indica and Japonica subpopulations.

Different approaches have been used to study genotype-environment associations, including mixed models (Coop et al., 2010; Lasky et al., 2014), generalized linear models (GLMs; Luo et al., 2021), and non-parametric approaches (Hancock et al., 2011; Pluess et al., 2016). We used TASSEL 5.0 (Bradbury et al., 2007) for our GWA analysis. After model evaluation, we used a GLM containing a correction for population structure, using the first five components as the population structure

matrix (GLM+PCA; Zhao et al., 2018; Supplemental Figure 8; Supplemental Document 2).

Using the “stats” package in R (R Core Team, 2020), we calculated the Benjamini–Hochberg (Benjamini and Hochberg, 1995) and Bonferroni (Holm, 1979) values for genome-wide significance to evaluate significance thresholds for multiple tests for each G-by-E association in our GWA analysis.

To predict the effect of every genetic variant, we used SnpEff (Cingolani et al., 2012) with gene model annotations from the Ensembl genome release 53 (<https://ftp.ensemblgenomes.ebi.ac.uk/pub/plants/release-53/>). We focused on SNPs within transcriptional units, including introns, 5' and 3' UTRs, and 1-kb promoter regions upstream of the most distal transcription start site. We used the “consensus transcript,” as described by SnpEff, as the variant with either the longest coding sequence if the gene had translated transcripts or the longest cDNA (Hubbard et al., 2009; Cingolani et al., 2012). We defined “common variants” as those with MAF $\geq 5\%$ to restrict our analysis to genetic variation that is more likely to be adaptive (Sawyer and Hartl, 1992; Ohta, 2005).

Genomic signatures of selection were calculated using VCFtools (Danecek et al., 2011). We obtained the fixation index, Fst (Wright, 1965; Weir and Cockerham, 1984), on a per-site basis and the genetic group based on Indica vs. Japonica cultivars. We also calculated nucleotide diversity (π) and Tajima's D in 1-kb windows across the genome (Danecek et al., 2011).

RiboSNitch prediction

A riboSNitch is a SNP that alters the secondary structure of an RNA. To identify riboSNitches in the rice transcriptome, we used the SNPfold software tool (Halvorsen et al., 2010). SNPfold predicts riboSNitches using a thermodynamic model that calculates the partition function and base-pairing probability matrices for the reference and variant sequences defined by any given SNP. SNPfold then compares the column sums of the base-pairing probability matrices by computing the Pearson correlation coefficient. A low SNPfold score, and thus a low Pearson correlation coefficient, indicates a potential structural change in the RNA, i.e., a riboSNitch. We suggest that SNPs are candidate riboSNitches if the correlation coefficient comparing the reference and variant sequences is less than 0.8 (Halvorsen et al., 2010), but in Oryza CLIMtools, we provide the specific SNPfold score (correlation coefficient) for each predicted variant, enabling users to choose their own threshold for designating a SNP as a riboSNitch.

SNPfold was used to predict the presence of riboSNitches within the 3 914 483 natural genetic variants among the 658 Indica landrace varieties and 2 835 066 genetic variants among the 283 Japonica landrace varieties studied here. Each SNP in these transcriptomes was placed in the context of its surrounding 80 nucleotides (40 upstream and 40 downstream) and passed through the SNPfold program to determine the effect of the mutation on the local RNA structure. In Oryza CLIMtools, correlation coefficients are provided for all SNPs within annotated transcribed regions unless the SNP is located less than 40 nucleotides from a transcript end, in which case the correlation coefficient was not

calculated. SNPs located less than 40 nucleotides from either end of a transcript are designated as not applicable in Oryza CLIMtools.

Oryza GenoCLIM

Oryza GenoCLIM is a user-friendly Shiny (Chang et al., 2015a) component of Oryza CLIMtools. GenoCLIM is a searchable database generated with the DT package (Xie, 2016). For any locus ID, it provides information on the genetic variants found to be significantly associated (FDR < 0.01) with each of the 413 geoenvironmental variables included in this study. FDR thresholds are calculated for each individual environmental variable. This tool enables the user to search for a locus identifier of any given gene annotated using the Rice Annotation Project (RAP annotation; Sakai et al., 2013) and retrieve, if present, any association between the genetic variation (SNPs and indels) in that gene and any environmental variable(s) described in this study.

The database provides climate associations of genetic variants, and the user can query their gene of interest within the Indica or Japonica varieties in an interactive database. The results can be filtered according to different FDR thresholds and sorted on the basis of their association score or any of the other population genetic indicators provided for these associations. In addition, Oryza GenoCLIM provides a plot generated by Plotly (Sievert et al., 2018) that enables users to visualize the results interactively.

Oryza CLIMGeno

Oryza CLIMGeno comprises a software suite of Shiny apps (Chang et al., 2015a) for analyzing the relationships between genetic variation and environmental factors in rice. CLIMGeno is built on Zbrowse (Ziegler et al., 2015), a genome browser tool. Using CLIMGeno, users can visualize the top 2500 genetic variants (SNPs and indels) associated with each of the 413 environmental variables analyzed in this study. Specifically, the tool displays the highest-scoring variants in Indica (658) or Japonica (283) rice varieties.

In Oryza CLIMGeno, the “manage” tab provides users with a dropdown menu with which to select an environmental variable of interest. The tool then automatically generates a list of the 2500 genetic variants (SNPs and indels) with the strongest association score that have an FDR < 0.01 for that variable. Users can navigate to the “data table” tab to select and sort genetic variation based on various details such as position, allele frequency, locus identification, locus description, riboSNitch prediction, or SNP effect.

The “whole-genome view” tab displays an interactive Manhattan plot that represents the genetic variation associated with the geo-climatic variable previously selected in the “whole-genome view” tab. The x axis shows each of the 12 rice chromosomes, and the y axis displays the score (negative logarithm of the p value), depicting the strength of the association between genetic variability and any given environmental variable. Users can then select which genetic variants to display based on their predicted effect using the “select effect” box. Hovering over the data points reveals information on the genetic effect of a given genetic variant.

Oryza CLIMtools

Clicking on a genetic variant takes users to the “chromosome view” tab, which displays two Manhattan plots corresponding to the chromosome where the selected variant is located. The top plot enables users to browse genetic variation on that chromosome and zoom in on any given region. The bottom plot combines a Manhattan plot with an interactive display and annotation of genes found in the region of interest according to the gene model annotation from the Ensembl genome release (<https://ftp.ensemblgenomes.ebi.ac.uk/pub/plants/release-53/>). Users can explore the region of the chromosome surrounding the genetic variant(s) of interest by selecting a window size or using the menu on the left. Lastly, the “annotations table” tab provides an interactive table with annotation information on the region of interest selected on the Manhattan plot, complemented by a graphical annotation display.

Plant growth conditions and physiological characterization of drought tolerance in the *OsRGA1* mutant *d1*

Wild-type and *d1* mutants were grown in a greenhouse in two-gallon pots containing Metro-Mix 360 potting mixture. Greenhouse temperatures were maintained at 30°C during the day and 20°C at night with a 16:8-h day/night cycle; light was supplied as natural daylight supplemented with 1000-W metal halide lamps (Philips Lighting, Somerset, NJ) for the duration of the light cycle. Photosynthetic photon flux density (PPFD) was \sim 500 $\mu\text{mol m}^{-2} \text{s}^{-1}$. Plants were maintained under well-watered conditions until 60 days after emergence. At that point, we introduced two drought treatments, which resulted in moderate or severe stress. Plants were watered twice daily to maintain at all times, by lysimetry, the three water treatments: well-watered/no drought (100% soil relative water content [SRWC]), moderate drought (45% SRWC), and severe drought (30% SRWC). There were seven replicates per water treatment per genotype, for a total of 42 plants. SRWC was kept constant from the start of the drought treatment until seed maturity by continued twice-daily watering to the appropriate weight and continuous monitoring with a Campbell Scientific TDR 100 system (Campbell Scientific, Logan, UT) using a custom-made probe of 20-cm length. The SRWC did not vary more than 5% between watering events.

For gas-exchange measurements, regions of flag leaves were enclosed in the chamber of a portable gas-exchange system (LI-COR 6400 IRGA with an integrated 6400-40 leaf chamber fluorometer; LI-COR, Lincoln, NE). Leaves were measured at the point of maximal width. The leaf chamber temperature was kept constant at 30°C. Airflow in the chamber was adjusted to 300 $\mu\text{mol s}^{-1}$. Steady-state measurements of different physiological parameters were performed at 500 $\mu\text{mol m}^{-2} \text{s}^{-1}$ PPFD provided by the Li-COR red/blue LED system, with blue light accounting for 10% of the total photon flux.

Amplification of G protein subunits

The G protein subunits of rice are encoded by *OsRGA1* (Os05g0333200), *OsXLG1* (Os12g0593000), *OsXLG3a* (Os11g0206700), *OsXLG3b* (Os06g0111400), *OsXLG4* (Os10g0117800), *OsRGB1* (Os03g0669200), *OsRGG1* (Os03g0635100), *OsRGG2* (Os02g0137800), *OsGS3* (Os03g0407400), *OsDEP1* (Os09g0441900), and *OsGGC2* (Os08g0456600). G protein subunit ORFs were amplified from seedling or flower cDNA of the Japonica Tai-

Plant Communications

chung 65 variety and cloned into the pCR8/GW/TOPO entry vector (Thermo). The 5' end of the *OsXLG4* ORF includes partially repetitive regions of >80% GC content and could not be amplified from cDNA. To circumvent this issue, the region of the *OsXLG4* cDNA encoding amino acids 198–828 was amplified from Tai-chung 65 cDNA and joined by overlap extension PCR to a gBlock fragment (IDT) of the region encoding amino acids 1–197 that was designed to encode the correct amino acids with reduced GC content. Overlap extension PCR was used to generate previously described deletions of *OsGS3* (*OsGS3-4*, *OsGS3-5*, *OsGS3-7*), and an *OsGS3-3* clone was created by incorporating the C55* mutation (chromosome 3, position 16 733 441) into a 3' primer that only amplified the shortened ORF of the *OsGS3-3* allele. *OsGS3-6*, *Osdep1*, and *OsDn1-1* were cloned by a method similar to that used for *OsGS3-3* (see [Supplemental Table 3](#) for primers used). The *OsGS3-3* and *OsGS3-4* alleles were originally named by [Mao et al. \(2010\)](#). We continued this naming convention with the alleles described by [Takano-Kai et al. \(2013\)](#), i.e., *OsGS3-5* corresponds to the allele identified in the Podiwi-A8 cultivar, *OsGS3-6* to the allele from JC73-4, JC157, and ABRI, *OsGS3-7* to the allele from H343 and Tumo-Tumo, and the allele identified in ARC7291 and TAL214 cultivars to the already described *OsGS3-4* allele ([Mao et al., 2010](#)) identified in the Chuan 7 cultivar ([Fan et al., 2006](#)). *Osdep1* was described by [Huang et al. \(2009\)](#) and *OsDn1-1* by [Taguchi-Shiobara et al. \(2011\)](#). Multiple alignments of the protein sequences of the above *OsGS3* and *OsDEP1* alleles were constructed using Clustal Omega ([Nguyen et al., 2016](#)).

Yeast protein–protein interaction assays

Sequence-verified Gateway entry clones were mobilized into pDEST-GADT7 and pDEST-GBKT7 destination yeast two-hybrid vectors ([Uetz et al., 2006](#)) by Gateway LR recombination. For yeast three-hybrid assays, in which the interaction of two proteins is assayed by a yeast two-hybrid approach in the presence of a third “bridge” protein, *OsRGB1* was amplified with flanking NotI and BamHI sites and cloned into the NotI/BgIII sites of pBridge MCS2 (Takara) as the “bridge” protein. G γ subunits were amplified with flanking BgIII sites for ligation into the compatible BamHI site (*OsGS3* alleles) or with EcoRI and Sall restriction sites (*OsRGG1*, *OsRGG2*, *OsGGC2*) or EcoRI and BamHI restriction sites (*OsDEP1* alleles) for cloning into MCS1 of pBridge as GAL4BD fusions. Yeast two- and three-hybrid assays were performed as described previously ([Chakravorty et al., 2015](#)).

DATA AND CODE AVAILABILITY

For reproducibility, the source code and data used in Oryza CLIMtools are freely available for download at GitHub (<https://github.com/CLIMtools>), with code licensed under Apache 2.0.

SUPPLEMENTAL INFORMATION

Supplemental information is available at *Plant Communications Online*.

FUNDING

This work was supported by the National Institute of General Medical Sciences of the NIH under award number 5R01GM126079 to S.M.A. and NSF-IOS-2122357 to Prof. Philip C. Bevilacqua and S.M.A. K.J.K. acknowledges support from NIH training grant 5T32GM102057.

AUTHOR CONTRIBUTIONS

A.F.-S. and S.M.A. conceived the project. D.C. designed, performed, and analyzed the yeast protein–protein interaction assays. K.J.K. performed the riboSNitch predictions. A.F.-S. assembled Oryza CLIMtools and performed all other computational analyses. A.F.-S. characterized drought tolerance and performed gas-exchange analysis in the *OsRGA1* mutant *d1*. A.F.-S., along with S.M.A. and D.C., wrote the manuscript, which incorporated key comments from K.J.K. All authors read and approved the final manuscript.

ACKNOWLEDGMENTS

The content is solely the responsibility of the authors and does not necessarily represent the official views of the NIH. We thank Prof. D. Ware, Dr. A. Olson, and Prof. P.C. Bevilacqua for helpful discussions and comments on this manuscript. We also thank the Gramene Team (<https://www.gramene.org/>) for hosting Oryza CLIMtools. The Pennsylvania State University has a patent (US9434957B2), authored by S.M.A., A.F.-S., and D.C., on the manipulation of RGA1 activity to engineer drought tolerance and improved seed production in plants. No conflict of interest declared.

Received: July 15, 2023

Revised: October 12, 2023

Accepted: January 5, 2024

Published: January 11, 2024

REFERENCES

3,000 rice genomes project. (2014). The 3,000 rice genomes project. *GigaScience* 3:7.

Ashikari, M., Wu, J., Yano, M., Sasaki, T., and Yoshimura, A. (1999). Rice gibberellin-insensitive dwarf mutant gene *Dwarf 1* encodes the α -subunit of GTP-binding protein. *Proc. Natl. Acad. Sci. USA* 96:10284–10289.

Benjamini, Y., and Hochberg, Y. (1995). Controlling the false discovery rate: A practical and powerful approach to multiple testing. *J. R. Stat. Soc.* 57:289–300.

Bin Rahman, A.N.M.R., and Zhang, J. (2023). Trends in rice research: 2030 and beyond. *Food Energy Secur.* 12:e390.

Botella, J.R. (2012). Can heterotrimeric G proteins help to feed the world? *Trends Plant Sci.* 17:563–568.

Bradbury, P.J., Zhang, Z., Kroon, D.E., Casstevens, T.M., Ramdoss, Y., and Buckler, E.S. (2007). TASSEL: software for association mapping of complex traits in diverse samples. *Bioinformatics* 23:2633–2635.

Browning, B.L., Zhou, Y., and Browning, S.R. (2018). A one-penny imputed genome from next-generation reference panels. *Am. J. Hum. Genet.* 103:338–348.

Cantos, C.F., dePamphilis, C.W., and Assmann, S.M. (2023). Extra-large G proteins have extra-large effects on agronomic traits and stress tolerance in maize and rice. *Trends Plant Sci.* Advance Access. published.

Casañas, F., Simó, J., Casals, J., and Prohens, J. (2017). Toward an evolved concept of landrace. *Front. Plant Sci.* 8:145.

Chakravorty, D., Trusov, Y., Zhang, W., Acharya, B.R., Sheahan, M.B., McCurdy, D.W., Assmann, S.M., and Botella, J.R. (2011). An atypical heterotrimeric G-protein γ -subunit is involved in guard cell K-channel regulation and morphological development in *Arabidopsis thaliana*. *Plant J.* 67:840–851.

Chakravorty, D., Gookin, T.E., Milner, M.J., Yu, Y., and Assmann, S.M. (2015). Extra-large G proteins expand the repertoire of subunits in *Arabidopsis* heterotrimeric G protein signaling. *Plant Physiol.* 169:512–529.

Chang, W., Cheng, J., Allaire, J., Xie, Y., and McPherson, J. (2015a). Shiny: Web Application Framework for R. R Package Version 1.6.0. <https://cran.r-project.org/web/packages/shiny/index.htm>.

Chang, C.C., Chow, C.C., Tellier, L.C., Vattikuti, S., Purcell, S.M., and Lee, J.J. (2015b). Second-generation PLINK: rising to the challenge of larger and richer datasets. *GigaScience* 4:7.

Chaya, G., Segami, S., Fujita, M., Morinaka, Y., Iwasaki, Y., and Miura, K. (2022). OsGGC2, G γ subunit of heterotrimeric G protein, regulates plant height by functionally overlapping with *DEP1* in Rice. *Plants (Basel.)*, *Plants* 11:422.

Cingolani, P., Platts, A., Wang, L.L., Coon, M., Nguyen, T., Wang, L., Land, S.J., Lu, X., and Ruden, D.M. (2012). A Program for Annotating and Predicting the Effects of Single Nucleotide Polymorphisms, SnpEff: SNPs in the Genome of *Drosophila melanogaster* Strain W1118. *iso-2; iso-3*. 6:80–92.

Coop, G., Witonsky, D., Di Rienzo, A., and Pritchard, J.K. (2010). Using environmental correlations to identify loci underlying local adaptation. *Genetics* 185:1411–1423.

Cui, Y., Jiang, N., Xu, Z., and Xu, Q. (2020). Heterotrimeric G protein are involved in the regulation of multiple agronomic traits and stress tolerance in rice. *BMC Plant Biol.* 20:90.

Dalrymple, D.G. (1986). Development and spread of high-yielding rice varieties in developing countries. *Int. Rice Res. Inst.*

Danecek, P., Auton, A., Abecasis, G., Albers, C.A., Banks, E., DePristo, M.A., Handsaker, R.E., Lunter, G., Marth, G.T., Sherry, S.T., et al. (2011). The variant call format and VCFtools. *Bioinformatics* 27:2156–2158.

Delmotte, V., Zhai, P., Pörtner, H.O., Roberts, D., Skea, J., Shukla, P.R., Pirani, A., Okia, W.M., Péan, C., Pidcock, R., et al. (2018). Global warming of 1.5°C. An IPCC Special Report on the impacts of global warming of 1.5°C above pre-industrial levels and related global greenhouse gas emission pathways, in the context of strengthening the global response to the threat of climate change, sustainable development, and efforts to eradicate poverty. In Report of the Intergovernmental Panel on Climate Change.

Fan, C., Xing, Y., Mao, H., Lu, T., Han, B., Xu, C., Li, X., and Zhang, Q. (2006). GS3, a major QTL for grain length and weight and minor QTL for grain width and thickness in rice, encodes a putative transmembrane protein. *Theor. Appl. Genet.* 112:1164–1171.

Farooq, M., Hussain, M., Wahid, A., and Siddique, K.H.M. (2012). Drought stress in plants: an overview. In *Plant Responses to Drought Stress: From Morphological to Molecular Features*, R. Aroca, ed. 1–33 (Springer Berlin Heidelberg).

Faye, J.M., Maina, F., Hu, Z., Fonceka, D., Cisse, N., and Morris, G.P. (2019). Genomic signatures of adaptation to Sahelian and Soudanian climates in sorghum landraces of Senegal. *Ecol. Evol.* 9:6038–6051.

Ferrero-Serrano, Á., and Assmann, S.M. (2016). The α -subunit of the rice heterotrimeric G protein, *RGA1*, regulates drought tolerance during the vegetative phase in the dwarf rice mutant *d1*. *J. Exp. Bot.* 67:3433–3443.

Ferrero-Serrano, Á., and Assmann, S.M. (2019). Phenotypic and genome-wide association with the local environment of *Arabidopsis*. *Nat. Ecol. Evol.* 3:274–285.

Ferrero-Serrano, Á., and Chakravorty, D. (2023). Plants and heterotrimeric G proteins: Expect the unexpected. *Mol. Plant* 16:506–508.

Ferrero-Serrano, Á., Su, Z., and Assmann, S.M. (2018). Illuminating the role of the G α heterotrimeric G protein subunit, RGA1, in regulating photoprotection and photoavoidance in rice. *Plant Cell Environ.* 41:451–468.

Oryza CLIMtools

Ferrero-Serrano, Á., Cantos, C., and Assmann, S.M. (2019). The role of dwarfing traits in historical and modern agriculture with a focus on rice. *Cold Spring Harb. Perspect. Biol.* **11**.

Ferrero-Serrano, Á., Sylvia, M.M., Forstmeier, P.C., Olson, A.J., Ware, D., Bevilacqua, P.C., and Assmann, S.M. (2022). Experimental demonstration and pan-structure prediction of climate-associated riboSNitches in *Arabidopsis*. *Genome Biol.* **23**:101.

Fitter, A.H., and Fitter, R.S.R. (2002). Rapid changes in flowering time in British plants. *Science* **296**:1689–1691.

Food and Agriculture Organization of the United Nations, United Nations International Children's Emergency Fund, World Health Organization, World Food Programme, and International Fund for Agriculture Development. (2018). The State of Food Security and Nutrition in the World 2018: Building Climate Resilience for Food Security and Nutrition (Food & Agriculture Org.).

Frankel, O.H. (1974). Genetic conservation: our evolutionary responsibility. *Genetics* **78**:53–65.

Fu, Y.-B., and Somers, D.J. (2009). Genome-wide reduction of genetic diversity in wheat breeding. *Crop Sci.* **49**:161–168.

Garris, A.J., Tai, T.H., Coburn, J., Kresovich, S., and McCouch, S. (2005). Genetic structure and diversity in *Oryza sativa* L. *Genetics* **169**:1631–1638.

Godfray, H.C.J., Beddington, J.R., Crute, I.R., Haddad, L., Lawrence, D., Muir, J.F., Pretty, J., Robinson, S., Thomas, S.M., and Toulmin, C. (2010). Food security: the challenge of feeding 9 billion people. *Science* **327**:812–818.

Guo, T., Mu, Q., Wang, J., Vanous, A.E., Onogi, A., Iwata, H., Li, X., and Yu, J. (2020). Dynamic effects of interacting genes underlying rice flowering-time phenotypic plasticity and global adaptation. *Genome Res.* **30**:673–683.

Gupta, A., Rico-Medina, A., and Caño-Delgado, A.I. (2020). The physiology of plant responses to drought. *Science* **368**:266–269.

Gutaker, R.M., Groen, S.C., Bellis, E.S., Choi, J.Y., Pires, I.S., Bocinsky, R.K., Slayton, E.R., Wilkins, O., Castillo, C.C., Negrão, S., et al. (2020). Genomic history and ecology of the geographic spread of rice. *Nat. Plants* **6**:492–502.

Halvorsen, M., Martin, J.S., Broadaway, S., and Laederach, A. (2010). Disease-associated mutations that alter the RNA structural ensemble. *PLoS Genet.* **6**:e1001074.

Han, Z., Zhang, B., Zhao, H., Ayaad, M., and Xing, Y. (2016). Genome-wide association studies reveal that diverse heading date genes respond to short and long day lengths between Indica and Japonica rice. *Front. Plant Sci.* **7**:1270.

Hancock, A.M., Brachi, B., Faure, N., Horton, M.W., Jarymowycz, L.B., Sperone, F.G., Toomajian, C., Roux, F., and Bergelson, J. (2011). Adaptation to climate across the *Arabidopsis thaliana* genome. *Science* **334**:83–86.

Hargreaves, G.H., and Samani, Z.A. (1982). Estimating potential evapotranspiration. *J. Irrig. Drain. Div.* **108**:225–230.

Hargrove, T.R., and Cabanilla, V.L. (1979). The impact of semidwarf varieties on Asian rice-breeding programs. *Bioscience* **29**:731–735.

Hargrove, T.R., Coffman, W.R., and Cabanilla, V.L. (1980). Ancestry of improved cultivars of Asian rice 1. *Crop Sci.* **20**:721–727.

Hijmans, R.J., Van Etten, J., Mattiuzzi, M., Sumner, M., Greenberg, J.A., Lamigueiro, O.P., Bevan, A., Racine, E.B., and Shortridge, A. (2013). Raster: Geographic Data Analysis and Modeling. R package version 2.0. <https://cran.r-project.org/web/packages/raster/raster.pdf>.

Hoisington, D., Khairallah, M., Reeves, T., Ribaut, J.M., Skovmand, B., Taba, S., and Warburton, M. (1999). Plant genetic resources: what can they contribute toward increased crop productivity? *Proc. Natl. Acad. Sci. USA* **96**:5937–5943.

Plant Communications

Holm, S. (1979). A Simple Sequentially Rejective Multiple Test Procedure. *Scand. Stat. Theory Appl.* **6**:65–70.

Huang, X., Qian, Q., Liu, Z., Sun, H., He, S., Luo, D., Xia, G., Chu, C., Li, J., and Fu, X. (2009). Natural variation at the *DEP1* locus enhances grain yield in rice. *Nat. Genet.* **41**:494–497.

Huang, X., Kurata, N., Wei, X., Wang, Z.-X., Wang, A., Zhao, Q., Zhao, Y., Liu, K., Lu, H., Li, W., et al. (2012). A map of rice genome variation reveals the origin of cultivated rice. *Nature* **490**:497–501.

Hubbard, T.J.P., Aken, B.L., Ayling, S., Ballester, B., Beal, K., Bragin, E., Brent, S., Chen, Y., Clapham, P., Clarke, L., et al. (2009). Ensembl 2009. *Nucleic Acids Res.* **37**:D690–D697.

Jagadish, S.V.K., Muthurajan, R., Oane, R., Wheeler, T.R., Heuer, S., Bennett, J., and Craufurd, P.Q. (2010). Physiological and proteomic approaches to address heat tolerance during anthesis in rice (*Oryza sativa* L.). *J. Exp. Bot.* **61**:143–156.

Jangam, A.P., Pathak, R.R., and Raghuram, N. (2016). Microarray analysis of rice *d1* (*RGA1*) mutant reveals the potential role of G-protein alpha Subunit in regulating multiple abiotic stresses such as drought, salinity, heat, and cold. *Front. Plant Sci.* **7**:11.

Kajiya-Kanegae, H., Ohyanagi, H., Ebata, T., Tanizawa, Y., Onogi, A., Sawada, Y., Hirai, M.Y., Wang, Z.-X., Han, B., Toyoda, A., et al. (2021). OryzaGenome2.1: database of diverse genotypes in Wild Oryza Species. *Rice* **14**:24.

Karger, D.N., Conrad, O., Böhner, J., Kawohl, T., Kreft, H., Soria-Auza, R.W., Zimmermann, N.E., Linder, H.P., and Kessler, M. (2017). Climatologies at high resolution for the earth's land surface areas. *Sci. Data* **4**:170122–20.

Kato, S. (1930). On the affinity of the cultivated varieties of rice plants, *Oryza sativa* L. *Journal of the Department of Agriculture, Hokkaido Imperial University* **22** (3):121–198.

Khapho-Burch, M., Cooper, M., Crossa, J., de Leon, N., Holland, J., Lewis, R., McCouch, S., Murray, S.C., Rabbi, I., Ronald, P., et al. (2023). Genetic modification can improve crop yields—but stop overselling it. *Nature* **621**:470–473.

Khoury, C.K., Brush, S., Costich, D.E., Curry, H.A., de Haan, S., Engels, J.M.M., Guarino, L., Hoban, S., Mercer, K.L., Miller, A.J., et al. (2022). Crop genetic erosion: understanding and responding to loss of crop diversity. *New Phytol.* **233**:84–118.

Khush, G.S. (1997). Origin, dispersals, cultivation and variation of rice. In *Oryza: From Molecule to Plant*, T. Sasaki and G. Moore, eds. (Springer Netherlands), pp. 25–34.

Kong, F.N., Wang, J.Y., Zou, J.C., Shi, L.X., De Jin, M., Xu, Z.J., and Wang, B. (2007). Molecular tagging and mapping of the erect panicle gene in rice. *Mol. Breed.* **19**:297–304.

Koo, B.-H., Yoo, S.-C., Park, J.-W., Kwon, C.-T., Lee, B.-D., An, G., Zhang, Z., Li, J., Li, Z., and Paek, N.-C. (2013). Natural variation in *OsPRR37* regulates heading date and contributes to rice cultivation at a wide range of latitudes. *Mol. Plant* **6**:1877–1888.

Lasky, J.R., Des Marais, D.L., Lowry, D.B., Povolotskaya, I., McKay, J.K., Richards, J.H., Keitt, T.H., and Juenger, T.E. (2014). Natural variation in abiotic stress responsive gene expression and local adaptation to climate in *Arabidopsis thaliana*. *Mol. Biol. Evol.* **31**:2283–2296.

Lasky, J.R., Upadhyaya, H.D., Ramu, P., Deshpande, S., Hash, C.T., Bonnette, J., Juenger, T.E., Hyma, K., Acharya, C., Mitchell, S.E., et al. (2015). Genome-environment associations in sorghum landraces predict adaptive traits. *Sci. Adv.* **1**:e1400218.

Li, X., Liu, H., Wang, M., Liu, H., Tian, X., Zhou, W., Lü, T., Wang, Z., Chu, C., Fang, J., and Bu, Q. (2015). Combinations of *Hd2* and *Hd4* genes determine rice adaptability to Heilongjiang Province, northern limit of China. *J. Integr. Plant Biol.* **57**:698–707.

Liu, X., Liu, H., Zhang, Y., He, M., Li, R., Meng, W., Wang, Z., Li, X., and Bu, Q. (2021). Fine-tuning flowering time via genome editing of upstream open reading frames of *Heading Date* 2 in rice. *Rice* **14**:59.

Luo, L., Tang, Z.-Z., Schoville, S.D., and Zhu, J. (2021). A comprehensive analysis comparing linear and generalized linear models in detecting adaptive SNPs. *Mol. Ecol. Resour.* **21**:733–744.

Mansueto, L., Fuentes, R.R., Borja, F.N., Detras, J., Abriol-Santos, J.M., Chebotarov, D., Sanciangco, M., Palis, K., Copetti, D., Poliakov, A., et al. (2017). Rice SNP-seek database update: new SNPs, indels, and queries. *Nucleic Acids Res.* **45**:D1075–D1081.

Mao, H., Sun, S., Yao, J., Wang, C., Yu, S., Xu, C., Li, X., and Zhang, Q. (2010). Linking differential domain functions of the GS3 protein to natural variation of grain size in rice. *Proc. Natl. Acad. Sci. USA* **107**:19579–19584.

Matsui, T., Omasa, K., and Horie, T. (2001). The difference in sterility due to high temperatures during the flowering period among Japonica-rice varieties. *Plant Prod. Sci.* **4**:90–93.

McCudden, C.R., Hains, M.D., Kimple, R.J., Siderovski, D.P., and Willard, F.S. (2005). G-protein signaling back to the future. *Cell. Mol. Life Sci.* **62**:551–577.

McNally, K.L., Childs, K.L., Bohnert, R., Davidson, R.M., Zhao, K., Ulat, V.J., Zeller, G., Clark, R.M., Hoen, D.R., Bureau, T.E., et al. (2009). Genomewide SNP variation reveals relationships among landraces and modern varieties of rice. *Proc. Natl. Acad. Sci. USA* **106**:12273–12278.

Nakagawa, H., Yamagishi, J., Miyamoto, N., Motoyama, M., Yano, M., and Nemoto, K. (2005). Flowering response of rice to photoperiod and temperature: a QTL analysis using a phenological model. *Theor. Appl. Genet.* **110**:778–786.

Nguyen, K., Guo, X., and Pan, Y. (2016). Multiple Biological Sequence Alignment: Scoring Functions, Algorithms and Evaluation (John Wiley & Sons).

Nilson, S.E., and Assmann, S.M. (2010). The alpha-subunit of the *Arabidopsis* heterotrimeric G protein, GPA1, is a regulator of transpiration efficiency. *Plant Physiol.* **152**:2067–2077.

Oki, K., Inaba, N., Kitano, H., Takahashi, S., Fujisawa, Y., Kato, H., and Iwasaki, Y. (2009). Study of novel *d1* alleles, defective mutants of the α subunit of heterotrimeric G-protein in rice. *Genes Genet. Syst.* **84**:35–42.

Ohta, T. (2005). Molecular Evolution: Nearly Neutral Theory. In Encyclopedia of Life Sciences (John Wiley & Sons, Ltd (Ed.)).

Østerberg, J.T., Xiang, W., Olsen, L.I., Edenbrandt, A.K., Vedel, S.E., Christiansen, A., Landes, X., Andersen, M.M., Pagh, P., Sandøe, P., et al. (2017). Accelerating the domestication of new crops: feasibility and approaches. *Trends Plant Sci.* **22**:373–384.

Penman, H.L., and Keen, B.A. (1997). Natural evaporation from open water, bare soil and grass. *Proc. R. Soc. Lond. A Math. Phys. Sci.* **193**:120–145.

Pluess, A.R., Frank, A., Heiri, C., Lalagüe, H., Vendramin, G.G., and Oddou-Muratorio, S. (2016). Genome-environment association study suggests local adaptation to climate at the regional scale in *Fagus sylvatica*. *New Phytol.* **210**:589–601.

R Core Team. (2020). R: A Language and Environment for Statistical Computing (R Foundation for Statistical Computing). <https://www.R-project.org/>.

Renard, D., and Tilman, D. (2019). National food production stabilized by crop diversity. *Nature* **571**:257–260.

Sakai, H., Lee, S.S., Tanaka, T., Numa, H., Kim, J., Kawahara, Y., Wakimoto, H., Yang, C.-C., Iwamoto, M., Abe, T., et al. (2013). Rice Annotation Project Database (RAP-DB): an integrative and interactive database for rice genomics. *Plant Cell Physiol.* **54**:e6.

Salomé, P.A., Weigel, D., and McClung, C.R. (2010). The role of the *Arabidopsis* morning loop components CCA1, LHY, PRR7, and PRR9 in temperature compensation. *Plant Cell* **22**:3650–3661.

Sawyer, S.A., and Hartl, D.L. (1992). Population genetics of polymorphism and divergence. *Genetics* **132**:1161–1176.

Seck, P.A., Diagne, A., Mohanty, S., and Wopereis, M.C.S. (2012). Crops that feed the world 7: Rice. *Food Secur.* **4**:7–24.

Shrestha, S., Mahat, J., Shrestha, J., K C, M., and Paudel, K. (2022). Influence of high-temperature stress on rice growth and development. A review. *Heliyon* **8**:e12651.

Sievert, C., Hocking, T., Chamberlain, S., Ram, K., Corvellec, M., and Despouy, P. (2018). Plotly for R. <https://plotly-r.com/>.

Sun, S., Wang, L., Mao, H., Shao, L., Li, X., Xiao, J., Ouyang, Y., and Zhang, Q. (2018). A G-protein pathway determines grain size in rice. *Nat. Commun.* **9**:851–11.

Sweeney, M., and McCouch, S. (2007). The complex history of the domestication of rice. *Ann. Bot.* **100**:951–957.

Taguchi-Shiobara, F., Kawagoe, Y., Kato, H., Onodera, H., Tagiri, A., Hara, N., Miyao, A., Hirochika, H., Kitano, H., Yano, M., and Toki, S. (2011). A loss-of-function mutation of rice *DENSE PANICLE 1* causes semi-dwarfness and slightly increased number of spikelets. *Breed. Sci.* **61**:17–25.

Takano-Kai, N., Jiang, H., Kubo, T., Sweeney, M., Matsumoto, T., Kanamori, H., Padukasahasram, B., Bustamante, C., Yoshimura, A., Doi, K., and McCouch, S. (2009). Evolutionary history of GS3, a gene conferring grain length in rice. *Genetics* **182**:1323–1334.

Takano-Kai, N., Jiang, H., Powell, A., McCouch, S., Takamure, I., Furuya, N., Doi, K., and Yoshimura, A. (2013). Multiple and independent origins of short seeded alleles of GS3 in rice. *Breed. Sci.* **63**:77–85.

Tello-Ruiz, M.K., Naithani, S., Gupta, P., Olson, A., Wei, S., Preece, J., Jiao, Y., Wang, B., Chougule, K., Garg, P., et al. (2021). Gramene 2021: harnessing the power of comparative genomics and pathways for plant research. *Nucleic Acids Res.* **49**:D1452–D1463.

Thornthwaite, C.W. (1948). An approach toward a rational classification of climate. *Geogr. Rev.* **38**:55–94.

Title, P.O., and Bemmels, J.B. (2018). ENVIREM: an expanded set of bioclimatic and topographic variables increases flexibility and improves performance of ecological niche modeling. *Ecography* **41**:291–307.

Trusov, Y., Chakravorty, D., and Botella, J.R. (2012). Diversity of heterotrimeric G-protein γ subunits in plants. *BMC Res. Notes* **5**:608.

Ueguchi-Tanaka, M., Fujisawa, Y., Kobayashi, M., Ashikari, M., Iwasaki, Y., Kitano, H., and Matsuoka, M. (2000). Rice dwarf mutant *d1*, which is defective in the α subunit of the heterotrimeric G protein, affects gibberellin signal transduction. *Proc. Natl. Acad. Sci. USA* **97**:11638–11643.

Uetz, P., Dong, Y.-A., Zeretzke, C., Atzler, C., Baiker, A., Berger, B., Rajagopala, S.V., Roupelieva, M., Rose, D., Fossum, E., et al. (2006). Herpesviral protein networks and their interaction with the human proteome. *Science* **311**:239–242.

Utsunomiya, Y., Samejima, C., Takayanagi, Y., Izawa, Y., Yoshida, T., Sawada, Y., Fujisawa, Y., Kato, H., and Iwasaki, Y. (2011). Suppression of the rice heterotrimeric G protein β -subunit gene, *RGB1*, causes dwarfism and browning of internodes and lamina joint regions. *Plant J.* **67**:907–916.

Wang, Y., and Botella, J.R. (2022). Heterotrimeric g protein signaling in abiotic stress. *Plants* **11**.

Oryza CLIMtools

Wang, W., Mauleon, R., Hu, Z., Chebotarov, D., Tai, S., Wu, Z., Li, M., Zheng, T., Fuentes, R.R., Zhang, F., et al. (2018). Genomic variation in 3,010 diverse accessions of Asian cultivated rice. *Nature* **557**:43–49.

Wang, C.-C., Yu, H., Huang, J., Wang, W.-S., Faruquee, M., Zhang, F., Zhao, X.-Q., Fu, B.-Y., Chen, K., Zhang, H.-L., et al. (2020). Towards a deeper haplotype mining of complex traits in rice with RFGB v2.0. *Plant Biotechnol. J.* **18**:14–16.

Weir, B.S., and Cockerham, C.C. (1984). Estimating F-statistic for the analysis of population structure. *Evolution* **38**:1358–1370.

Wolfenstetter, S., Chakravorty, D., Kula, R., Urano, D., Trusov, Y., Sheahan, M.B., McCurdy, D.W., Assmann, S.M., Jones, A.M., and Botella, J.R. (2015). Evidence for an unusual transmembrane configuration of AGG3, a class C G_γ subunit of *Arabidopsis*. *Plant J.* **81**:388–398.

Wright, S. (1965). The interpretation of population structure by F-statistics with special regard to systems of mating. *Evolution* **19**:395–420.

Wu, T.-Y., and Urano, D. (2018). Genetic and systematic approaches toward G protein-coupled abiotic stress signaling in plants. *Front. Plant Sci.* **9**:1378.

Wu, T.-Y., Krishnamoorthi, S., Boonyavas, K., Al-Darabsah, I., Leong, R., Jones, A.M., Ishizaki, K., Liao, K.-L., and Urano, D. (2022). G protein controls stress readiness by modulating transcriptional and metabolic homeostasis in *Arabidopsis thaliana* and *Marchantia polymorpha*. *Mol. Plant Advance Access published November 1:2022*.

Xie, Y. (2016). DT: A Wrapper of the JavaScript Library ‘DataTables’. <https://cran.r-project.org/package=DT>.

Yan, C.-J., Zhou, J.-H., Yan, S., Chen, F., Yeboah, M., Tang, S.-Z., Liang, G.-H., and Gu, M.-H. (2007). Identification and characterization of a major QTL responsible for erect panicle trait in japonica rice (*Oryza sativa* L.). *Theor. Appl. Genet.* **115**:1093–1100.

Yan, W., Liu, H., Zhou, X., Li, Q., Zhang, J., Lu, L., Liu, T., Liu, H., Zhang, C., Zhang, Z., et al. (2013). Natural variation in *Ghd7.1* plays an important role in grain yield and adaptation in rice. *Cell Res.* **23**:969–971.

Plant Communications

Ye, J., Niu, X., Yang, Y., Wang, S., Xu, Q., Yuan, X., Yu, H., Wang, Y., Wang, S., Feng, Y., and Wei, X. (2018). Divergent *Hd1*, *Ghd7*, and *DTH7* alleles control heading date and yield potential of Japonica rice in Northeast China. *Front. Plant Sci.* **9**:35.

Zait, Y., Ferrero-Serrano, Á., and Assmann, S.M. (2021). The α subunit of the heterotrimeric G protein regulates mesophyll CO₂ conductance and drought tolerance in rice. *New Phytol.* **232**:2324–2338.

Zhang, W., He, S.Y., and Assmann, S.M. (2008). The plant innate immunity response in stomatal guard cells invokes G-protein-dependent ion channel regulation. *Plant J.* **56**:984–996.

Zhang, Q., Chen, Q., Wang, S., Hong, Y., and Wang, Z. (2014). Rice and cold stress: methods for its evaluation and summary of cold tolerance-related quantitative trait loci. *Rice* **7**:24.

Zhang, H., Mittal, N., Leamy, L.J., Barazani, O., and Song, B.-H. (2017). Back into the wild—Apply untapped genetic diversity of wild relatives for crop improvement. *Evol. Appl.* **10**:5–24.

Zhang, J., Zhou, X., Yan, W., Zhang, Z., Lu, L., Han, Z., Zhao, H., Liu, H., Song, P., Hu, Y., et al. (2015). Combinations of the *Ghd7*, *Ghd8* and *Hd1* genes largely define the ecogeographical adaptation and yield potential of cultivated rice. *New Phytol.* **208**:1056–1066.

Zhao, C., Piao, S., Wang, X., Huang, Y., Ciais, P., Elliott, J., Huang, M., Janssens, I.A., Li, T., Lian, X., et al. (2016). Plausible rice yield losses under future climate warming. *Nat. Plants* **3**:16202.

Zhao, H., Mitra, N., Kanetsky, P.A., Nathanson, K.L., and Rebbeck, T.R. (2018). A practical approach to adjusting for population stratification in genome-wide association studies: principal components and propensity scores (PCAPS). *Stat. Appl. Genet. Mol. Biol.* **17**.

Ziegler, G.R., Hartsock, R.H., and Baxter, I. (2015). Zbrowse: an interactive GWAS results browser. *PeerJ Comput. Sci.* **1**:e3.

Zong, W., Ren, D., Huang, M., Sun, K., Feng, J., Zhao, J., Xiao, D., Xie, W., Liu, S., Zhang, H., et al. (2021). Strong photoperiod sensitivity is controlled by cooperation and competition among *Hd1*, *Ghd7* and *DTH8* in rice heading. *New Phytol.* **229**:1635–1649.